

14p

GCA-TR-73-1-N

A STUDY OF PLANETARY METEOROLOGY

by
George Ohring



FINAL REPORT

Contract No. NASW-2221

Prepared for
NATIONAL AERONAUTICS AND SPACE ADMINISTRATION
HEADQUARTERS

(NASA-CR-131266) A STUDY OF PLANETARY
METEOROLOGY Final Report (GCA Corp.)
52 p HC \$4.75 CSCI 03B

N73-20847

Unclas
G3/30 17269

GCA-TR-73-1-N

FINAL REPORT

For

A STUDY OF PLANETARY METEOROLOGY

Contract No. NASW-2221

Contracting Officer: J. B. Phillips, Jr.
Technical Monitor: Robert F. Fellows

January 1973

Prepared by

GCA CORPORATION
GCA TECHNOLOGY DIVISION
Bedford, Massachusetts

Principal Investigator: George Ohring

for

NATIONAL AERONAUTICS AND SPACE ADMINISTRATION
HEADQUARTERS
Washington, D.C.

TABLE OF CONTENTS

<u>Section</u>	<u>Title</u>	<u>Page</u>
	SUMMARY	1
I	INTRODUCTION	2
II	THE TEMPERATURE AND AMMONIA PROFILE IN THE JOVIAN ATMOSPHERE FROM INVERSION OF THE JOVIAN EMIS- SION SPECTRUM	3
	A. Introduction	3
	B. Background	4
	C. Inversion Techniques	5
	D. The Observations	13
	E. Results	15
	F. Conclusions	28
	REFERENCES	29
III	A TECHNIQUE TO DEDUCE THE MARTIAN ATMOSPHERIC TEMPERATURE AND WATER VAPOR PROFILES FROM ORBITER OBSERVATIONS OF THE PLANET'S IR LIMB RADIANCE PROFILE	31
	A. Introduction	31
	B. Theory	33
	C. Application to the Problem of Inferring the Martian Temperature Profile	41
	REFERENCES	49

A STUDY OF PLANETARY METEOROLOGY

by George Ohring
GCA Corporation, GCA Technology Division, Bedford, Mass.

SUMMARY

Two essentially independent pieces of research were completed during the contract period. Titles and abstracts of these two research efforts follow.

The Temperature and Ammonia Profile in the Jovian Atmosphere from Inversion of the Jovian Emission Spectrum

Inversion techniques developed for remote soundings of the earth's atmosphere by meteorological satellites are applied to the few earth based observations of the Jovian emission spectrum. With a minimum of assumptions, it is possible to obtain directly from the observed spectra the profiles of atmospheric temperature and ammonia abundance. The temperature profile is obtained from inversion of the radiances observed in the infrared bands of methane and hydrogen. With the use of the derived temperature profile, the ammonia abundance profile is obtained from radiances observed in the infrared and microwave absorption bands of ammonia. The temperature profile is characterized by a definite tropopause region with a temperature of about 115K and a stratospheric region in which the temperature slowly increases with altitude. The derived ammonia profile indicates the presence of a saturated ammonia layer with a base temperature of $\approx 140\text{K}$. It is concluded that inversion of infrared and microwave emission spectra provides a powerful technique for sounding the Jovian atmosphere, and that more accurate measurements should be obtained from fly-bys and earth based observations.

A Technique to Deduce the Martian Atmospheric Temperature and Water Vapor Profiles from Orbiter Observations of the Planet's IR Limb Radiance Profile

The concept is described of deducing the temperature and constituent profile of a planetary atmosphere from orbiter measurements of the planet's IR limb radiance profile. Expressions are derived for the weighting functions associated with the limb radiance profile for two infrared transmission models. Analysis of the weighting functions for the Martian atmosphere indicates that a limb radiance profile in the 15μ CO_2 band can be used to determine the Martian atmospheric temperature profile from 20 to 60 km. Simulation of the Martian limb radiance profile in the rotational water vapor band indicates that Martian water vapor mixing ratios can be inferred from limb radiance observations in a water vapor band.

SECTION I

INTRODUCTION

The primary objectives of the research contract were:

(1) To study the meteorology of the planet Jupiter, with particular emphasis on the deduction of the atmospheric temperature profile through analysis of available infrared and microwave observations of the planet's emission spectrum.

(2) To develop inversion techniques for inferring atmospheric temperature and constituent profiles of planetary atmospheres.

Work was performed on both of these topics, although the emphasis was placed on item (1). As a result of the work on item (1), temperature profiles have been derived for the Jovian atmosphere. In addition to the temperature profiles, it was also possible to derive profiles of the ammonia abundance. This work is summarized in Section II. The effort on item (2) was devoted to development of the equations for inferring the temperature and water vapor profiles of planetary atmospheres from orbiter observations of the planet's limb radiance profile in CO₂ and H₂O absorption bands. The feasibility of applying the technique to the Martian atmosphere has also been examined. This work is reviewed in Section III.

The work on both of these topics makes use of inversion techniques that are being used or will be used for deducing temperature and constituent profiles of the earth's atmosphere from meteorological satellite observations. The results indicate that these techniques are very useful for the general problem of remote sounding of other planetary atmospheres.

Efforts should be made to obtain more accurate observations of the Jovian emission spectrum in the infrared and microwave, and the feasibility of deducing the temperature and water vapor profiles of the Martian and Venusian atmospheres should be further examined. It is also suggested that the technique that was applied to determine the NH₃ abundance profile on Jupiter, be applied to the determination of the water vapor profile on Venus from existing microwave emission observations.

SECTION II

THE TEMPERATURE AND AMMONIA PROFILE IN THE JOVIAN ATMOSPHERE FROM INVERSION OF THE JOVIAN EMISSION SPECTRUM

A. Introduction

Taylor (1972) has recently suggested an experiment to measure the vertical temperature profile of the Jovian atmosphere by fly-by observations of the planet's infrared emission spectrum in the 7.5μ methane band. The temperature profile would be deduced from the spectrum with the use of inversion techniques that have been developed for satellite temperature soundings of the earth's atmosphere (Chahine, 1970; Smith, 1970). There is already available from earth based observations a measured spectrum for Jupiter for the region 2.8 to 14μ , which includes the 7.5μ methane band (Gillett et al., 1969). The observed spectrum also includes absorption bands due to hydrogen and ammonia. Both hydrogen and methane can be assumed to be uniformly mixed in the Jovian atmosphere, and relative abundance estimates are available for these gases (see, for example, McElroy, 1969). Hence, the observed radiances in both the methane and the hydrogen bands provide information on the temperature profile.

Ammonia is not uniformly mixed in the Jovian atmosphere; it appears to be saturated over at least a part of the atmosphere that has been observed spectroscopically (McElroy, 1969) and, hence, its mixing ratio probably varies considerably with height. Thus, unless the ammonia profile is known a priori, which it is not, observations in the ammonia band cannot be used for temperature inferences. But, if one can derive the temperature profile from the radiances observed in the methane and hydrogen absorption bands, then, in principle, one can use the radiances observed in the ammonia bands to derive an estimate of the ammonia profile. The problem is similar to that of deriving the water vapor profile in the earth's atmosphere from satellite observations of an infrared water vapor absorption band, given the temperature profile (see, for example, Smith, 1970). In addition to its absorption bands in the infrared region, ammonia has an absorption band in the microwave region centered near 1.25 cm. Earth based observation of the Jovian emission in this microwave band are also currently available (Law and Staelin, 1968; Wrixon et al., 1971) and can be used together with the infrared ammonia bands to estimate the Jovian ammonia profile.

In this report, we attempt to derive estimates of the temperature and ammonia profiles in the Jovian atmosphere from earth based observations of the planet's infrared and microwave emission, using inversion techniques developed for analyzing meteorological satellite spectra of the earth's atmosphere. Admittedly, the quality of the Jovian spectra is not as high as the satellite spectra of the earth's atmosphere. On the other

hand, our knowledge of the Jovian atmosphere is not as great as our knowledge of the earth's atmosphere, so that the accuracy demands of soundings of the Jovian atmosphere are not as severe.

B. Background

Much of our information on the composition and structure of the Jovian atmosphere derives from spectroscopic observations of the planet's reflection and emission spectra and theoretical model building. The observed reflection spectra can be the result of cloud reflection, and atmospheric absorption and scattering processes, and are difficult to interpret (see, for example, McElroy, 1969). However, it has been possible to obtain from such observations estimates of relative and absolute abundances of atmospheric gases and rotational temperatures using a reflecting layer analysis. The abundances derived from such an analysis refer to the abundances above some reflecting level; the rotational temperatures refer to some sort of effective temperature of the atmosphere above the reflecting level. From observations of the planet's emission at infrared and microwave wavelengths additional estimates of atmospheric temperatures have been derived. However, the altitudes to which these temperatures refer are uncertain.

Theoretical model building makes use of available observations and applicable theory to develop models of the atmosphere consistent with the observations. This type of activity has taken several forms. For example, Kuiper (1952) and, most recently, Owen (1969) have pieced together an atmospheric composition and structure model from observations made at many wavelengths together with certain assumptions on the temperature and ammonia profiles. Trafton (1967) and Trafton and Munch (1969) have computed radiative-convective equilibrium temperature profiles based upon observational evidence of atmospheric composition. Hogan et al. (1969) have computed radiative-convective equilibrium temperature profiles for a number of different boundary conditions and compared the emission spectrums for these profiles with the observed infrared and microwave spectrums. Wildey and Trafton (1971) have attempted to match infrared limb darkening observations of Jupiter in the 8-14 μ region with theoretical limb darkening curves computed for various assumptions on atmospheric composition and temperature. Wrixon et al. (1971) have compared their observed microwave spectrum with one computed for an assumed Jovian model atmosphere.

On the basis of the observational evidence and the results of the theoretical model building, the following general picture emerges. The Jovian atmosphere consists mainly of hydrogen and helium, with the hydrogen percentage being at least 67 percent, and the hydrogen abundance above the reflecting level being about 67 km-atm (McElroy, 1969). Estimates of the CH₄ abundance range from 30m atm to 150m atm, with a recommended value of 45m atm (McElroy, 1969). Ammonia is apparently saturated over part of the Jovian atmosphere. Ammonia abundances derived from analyses of the

6470Å band are 7×10^2 cm atm (Kuiper, 1952) and 1.2×10^3 cm atm (Owen, 1969). Abundances derived from analyses of ultraviolet observations yield an upper limit of $\sim 2 \times 10^{-3}$ cm atm, which refers to an effective reflecting level higher in the atmosphere (due to Rayleigh scattering) than does the abundance derived from the 6740Å band (Anderson et al., 1969). There are apparently two cloud layers present in the observable Jovian atmosphere (Danielson and Tomasko, 1969; Owen, 1969). The lower cloud appears to be dense and at a temperature of ~ 220 K with composition unknown; the upper cloud appears to be optically thin in the near and far infrared, composed of ammonia crystals, and at a temperature of ~ 150 K. Pressures at the lower cloud-top appear to be of the order of several atmospheres; at the upper cloud of the order of a fraction of an atmosphere.

It is interesting to note that, in much of the theoretical model building, and also in the interpretation of some of the spectral observations, the approach is one of determining which one of a number of different model atmospheres best satisfies a particular observation, or set of observations. This is a rather indirect way of arriving at estimates of the atmospheric models most consistent with a given observation. For the analysis of the infrared and microwave emission spectra, a more direct technique - inversion of the actual observations - can be applied to deduce the temperature and ammonia profiles as a function of pressure. From the temperature-pressure profile, the temperature and ammonia profiles versus relative height can be obtained. The techniques for accomplishing such inversions are described in the next section.

C. Inversion Techniques

Temperature inversion. - The observed radiance at wavenumber ν_i for an optically thick atmosphere, such as the Jovian atmosphere in the infrared, can be written as

$$N(\nu_i) = \int_0^1 B[\nu_i, T(p)] d\tau(\nu_i, p) \quad (1)$$

where $\tau(\nu_i, p)$ is the transmittance from the pressure level p to the effective top of the atmosphere, and B is the Planck function, given by

$$B(\nu, T) = c_1 \nu^3 / [\exp(c_2 \nu / T) - 1] \quad (2)$$

where T is the temperature and c_1 and c_2 are known constants. Our objective is to derive the temperature-pressure profile from observations of the radiances at n wavenumbers, given the distribution of the absorbing

gases, which determines the transmittances. Smith (1970) has derived an iterative technique for deriving the temperature profile from such observations. One starts with a guess temperature profile and iterates until some convergence criterion is achieved.

In an iterative form, equation (1) becomes

$$N(\nu_i) - N^j(\nu_i) = \int_0^1 \{B^{j+1}[\nu_i, T(p)] - B^j[\nu_i, T(p)]\} d\tau(\nu_i, p) \quad (3)$$

where j and $j+1$ represent the j th and $j+1$ iterations. $N(\nu_i)$ is the measured radiance and $N^j(\nu_i)$ is the radiance computed from equation (1) using the temperature profile at step j . For purposes of deriving the iteration technique it is assumed that for each wavenumber the difference of Planck functions within the integral is independent of pressure within the sensed atmospheric layer. Hence, the following iterative equation results

$$B^{j+1}(\nu_i, p) = B^j(\nu_i, p) + [N(\nu_i) - N^j(\nu_i)] \quad (4)$$

With the use of the Planck formula, it follows that an independent estimate of the temperature at the pressure level p can be obtained for each observing wavenumber from

$$T^{j+1}(\nu_i, p) = c_2 \nu_i / \ln \left[\frac{c_1 \nu_i^3 + B^{j+1}(\nu_i, p)}{B^{j+1}(\nu_i, p)} \right] \quad (5)$$

The best new estimate of the temperature at the pressure level p is given by the weighted average of the estimates from the n observed wavenumbers

$$T^{j+1}(p) = \sum_{i=1}^n T^{j+1}(\nu_i, p) W(\nu_i, p) / \sum_{i=1}^n W(\nu_i, p) \quad (6)$$

where, from equation (3), it follows that the weights should be

$$W(\nu_i, p) = d\tau(\nu_i, p) \quad (7)$$

The convergence criterion generally used in analyzing satellite observations of the earth's atmosphere is that

$$\left| N^{j+1}(\nu_i) - N^j(\nu_i) \right| / N(\nu_i) \leq \epsilon \quad i = 1, 2, \dots, n \quad (8)$$

where ϵ is a fraction of a percent. This value of ϵ is commensurate with the accuracies of the observations. For our analysis of the Jovian atmosphere spectrum, we used a different convergence criterion. The iterations were stopped when changes in temperature from one iteration step to the next were $\leq 0.5K$ at all atmospheric levels. The radiance observations in the infrared methane and hydrogen absorption bands are used in the inversion procedure.

Ammonia inversion.- We now turn to the problem of deriving the ammonia profile from the observed infrared and microwave radiances in the ammonia absorption bands. The temperature profile is assumed to be known from the temperature inversion procedure. By integrating equation (1) by parts, one can obtain

$$N(\nu_i) = B[\nu_i, T(p_0)] + \int_{B[\nu_i, T(p_0)]}^{B[\nu_i, T(p_r)]} \tau(\nu_i, p) dB[\nu_i, T(p)] \quad (9)$$

where p_0 is the effective top of the atmosphere for ammonia emission and p_r is a reference pressure deep in the atmosphere. In a manner similar to that used for deriving the temperature iteration equations, Smith (1970) shows that the abundance, a , of optically active gas above a pressure level p can be estimated at iteration step $j+1$ from

$$a^{j+1}(\nu_i, p) = a^j(p) \{1 + [N(\nu_i) - N^j(\nu_i)]/S^j\} \quad (10)$$

where

$$s^j = \int_{B[\nu_i, T(p_0)]}^{B[\nu_i, T(p_r)]} a^j(p) \left[\frac{\partial \tau(\nu_i, p)}{\partial a(p)} \right]^j dB[\nu_i, T(p)] \quad (11)$$

The best estimate of the abundance above the pressure level p is given by a weighted average of the abundances obtained from (10)

$$a^{j+1}(p) = \frac{\sum_{i=1}^m a^{j+1}(\nu_i, p) w^j(\nu_i, p)}{\sum_{i=1}^m w^j(\nu_i, p)} \quad (12)$$

where the weights are given by

$$w^j(\nu_i, p) = \left[\frac{\partial \tau(\nu_i, p)}{\partial a(p)} \right]^j dB(\nu_i, p) \quad (13)$$

and m is the number of wavenumbers for which radiances are observed.

Equation (13) is appropriate for an absorption band in a single spectral interval. For observations in which absorption bands in different parts of the emission spectrum are used in the inversion, the Planck function will vary considerably due to its wavenumber dependence. Hence, equation (13) would tend to weight more heavily observations at those wavenumbers near the peak of the Planck function at the expense of observations at the other wavenumbers. This is not desirable and we have removed this distortion by assuming that the weights are given by

$$w^j(\nu_i, p) = \left[\frac{\partial \tau(\nu_i, p)}{\partial a(p)} \right]^j \quad (14)$$

The iteration procedure is similar to that for the temperature profile. One starts with a guess distribution of ammonia abundance and

iterates until some convergence criterion is met. As opposed to the temperature profile inversion, however, the weights change from iteration to iteration since they are themselves determined by the ammonia profile. The convergence criterion adopted for the analysis of the Jovian ammonia radiances is

$$\left| \frac{[N^{j+1}(\nu_i) - N^j(\nu_i)]}{N^j(\nu_i)} \right| \leq \epsilon = 0.01 \quad i = 1, 2, \dots, m \quad (15)$$

Transmittance models.- To apply the inversion techniques, one needs transmittance functions for the absorption bands. For the 7.7μ band of CH_4 , we have followed McClatchey et al. (1970). McClatchey et al. present an empirical transmittance function in graphical form, from which we have derived an analytical representation of the transmittance

$$\tau(\nu, p) = \exp \{-[k_\nu L(p)]^{0.56}\} \quad (16)$$

where $\tau(\nu, p)$ is the transmittance of a 20 cm^{-1} interval centered at wave-number ν from the pressure level p to the top of the atmosphere; k_ν is the absorption coefficient for the interval; and L is a pressure corrected path length from the level p to the top of the atmosphere

$$L(p) = \frac{n_4}{1.75 A n} p^{1.75} \quad (17)$$

where n_4 is the CH_4 number density, n is the atmospheric number density, and

$$A = n_{\text{STP}} (p_s)^{0.75} \mu g \quad (18)$$

where n_{STP} is the number density at STP, p_s is standard pressure, μ is the mean molecular mass of the atmosphere, and g is the gravitational acceleration. Values of the absorption coefficients derived from this analysis are shown in Table 1. Further details may be found in Ohring (1971).

For the pressure induced absorption of hydrogen, we follow Trafton (1967). The transmittance is given by

TABLE 1

ABSORPTION COEFFICIENTS FOR THE 7.7 μ BAND OF METHANE

Wavenumber (cm^{-1})	Wavelength (μ)	k_{ν} (atm-cm) $^{-1}$
1160	8.6	5.4×10^{-3}
1200	8.3	6.2×10^{-3}
1220	8.2	1.7×10^{-2}
1240	8.1	1.1×10^{-1}
1260	7.9	6.2×10^{-1}
1280	7.8	9.4×10^{-1}

$$\tau(\nu, z) = \exp\left[-\int_z^{\infty} k_{\nu} dz\right] \quad (19)$$

where $\tau(\nu, z)$ is the transmittance from the height z to the top of the atmosphere, and k_{ν} is the volume absorption coefficient of H_2 , which, for a hydrogen helium mixture, can be written as

$$k_{\nu} = \frac{n_2^2}{c} \left[A_{\nu}(T) + qB_{\nu}(T) \right] \quad (20)$$

where n_2 is the hydrogen number density, c is the speed of light, q is the ratio of helium to hydrogen number densities, and $A_{\nu}(T)$ and $B_{\nu}(T)$ are the pressure induced binary absorption coefficients corresponding to absorption in pure H_2 and the enhancement in He- H_2 mixtures, respectively, at temperature T . Trafton and Munch (1969) and Trafton (1967) present graphs of A_{ν} and B_{ν} as a function of wavenumber for two different temperatures: $T = 160K$ and $T = 80K$. From these graphs we have derived the values of A_{ν} and B_{ν} for use in equation (20).

Two ammonia bands are present in the infrared spectrum observed by Gillett et al. (1969). For the 10.5μ NH_3 band, we follow Gille and Lee (1969), who calculated the positions, half-widths, and intensities of absorption lines due to NH_3 at $\nu < 1400 \text{ cm}^{-1}$, and used this information to calculate the parameters of the Goody random absorption model with exponential distribution of intensities. The transmittance for a spectral interval, $\Delta\nu$, 25 cm^{-1} wide, and centered at ν , from the height z to the top of the atmosphere can be written as

$$\tau_{\nu} = \exp \left\{ -\frac{\sigma_{\nu} a}{25} \left[\frac{a}{4} \frac{1}{\bar{P}_e \bar{f}} \left(\frac{\sigma_{\nu}}{\beta_{\nu}} \right)^2 + 1 \right]^{-1/2} \right\} \quad (21)$$

where a is the ammonia abundance above level z , \bar{P}_e is the mean effective pressure and \bar{f} the mean effective temperature along the path (for correcting for the pressure and temperature dependences of the half widths of the absorption lines), and values of σ_{ν} and β_{ν} are the parameters of the Goody random model. Values of σ_{ν} and β_{ν} are tabulated by Gille and Lee (1969) for a number of different temperatures. We have neglected the temperature dependence, which is relatively small for the temperature and wavenumber range of concern in the Jovian atmosphere, and have adopted Gille and Lee's

B

values of σ_ν and β_ν for a temperature of 150K. We have also adopted Gille and Lee's expressions for the effective pressure and temperature.

For the 6.1μ NH_3 band we have fit a strong line transmittance law to the laboratory observations of absorption by France and Williams (1966). The transmittance in the strong line approximation can be written as

$$\tau_\nu = \exp \left\{ - k_\nu [a \bar{P}_e \bar{f}]^{1/2} \right\} \quad (22)$$

It is assumed that \bar{P}_e and \bar{f} have the same forms as for the 10.5μ NH_3 band. Values of k_ν derived from this analysis are tabulated in Table 2. Unfortunately, the values of k_ν derived from this analysis must be considered very uncertain since the laboratory data include only one set of observations for NH_3 paths as large as 49 atm-cm, the remaining observations being for paths less than 3 atm-cm.

For absorption by ammonia in the microwave region, we follow Wrixon et al. (1971). In general, the ammonia absorption coefficient is given by (Townes and Schawlow, 1955)

$$k_\nu = \sum_{J=1}^{\infty} \sum_{K=1}^J 1.225 P_3 T^{-7/2} \times \frac{S(K) (2J+1) K^2}{J(J+1)} \times \exp \{-[2.98J(J+1) - 1.09K^2] 4.8/T\} F(\nu) \quad (23)$$

where k_ν is the absorption coefficient at frequency ν in units of cm^{-1} (note that for the microwave region ν represents frequency, not wavenumber), P_3 is the partial pressure of NH_3 in atmospheres, $S(K) = 3$ for K a multiple of 3, and $S(K) = 1.5$ otherwise, and $F(\nu)$ is the line shape factor. At low pressures ($p < 10$ cm Hg of pure NH_3), the absorption lines are distinct, and individual lines can be adequately represented by the Van Vleck-Weisskopf shape. As the pressure is increased, the individual lines are broadened and wiped out, and a single Van Vleck-Weisskopf expression can be used to express the absorption coefficient. As the pressure is further increased ($p > 30$ cm Hg of pure NH_3), the shape of the absorption spectrum changes from the resonant Van Vleck-Weisskopf form to the non-resonant Debye line shape (Bleaney and Loubser, 1950). Ben Reuven (1966) has derived a formula that approximates the absorption at these pressures. In the present study, we use the Van Vleck-Weisskopf shape - summing the individual lines as indicated by

TABLE 2
 ABSORPTION COEFFICIENTS FOR THE 6.1 μ BAND OF AMMONIA

Wavenumber (cm ⁻¹)	Wavelength (μ)	k_{ν}^2 (cm-atm ²) ^{-1/2}
1785	5.6	0.10
1850	5.4	0.023

equation (23) — at the upper levels (lower pressures) of the Jovian atmosphere, and Ben Reuven's formulation at the higher pressures. The change-over is made when the line widths in the Jovian atmosphere are equal to or greater than the line widths at a pressure of pure NH₃ of 30 cm Hg. The expressions for the Van Vleck-Weisskopf and Ben Reuven line shape factors given by Wrixon et al. (1971) were adopted for this study.

The transmittance at frequency ν from the level z to the top of the atmosphere is then given by

$$\tau_{\nu} = \exp \left[- \int_z^{\infty} k_{\nu}(z) dz \right] \quad (24)$$

D. The Observations

The infrared spectrum used in the present study is based upon the Gillett et al. (1969) observations of Jupiter over a period of five different nights. Observations were made in the 2.8-5.6 μ and the 7.4-15 μ regions with a resolution of $\Delta\lambda/\lambda \approx 0.02$. The observations were combined into the single spectrum shown in Figure 1. Statistical errors in the observations can be judged by the vertical spread of adjacent points.

For $\lambda < 4\mu$, Gillett et al. assume that reflected and scattered sunlight is the primary source of the radiation; for $\lambda > 5\mu$ they assume that thermal emission from Jupiter is the primary source. The shape of the spectrum at $\lambda > 5\mu$ can be attributed to ammonia bands in the regions 5.2 - 5.6 μ and 9 - 12 μ ; to a methane band in the region 7.8 - 8.4 μ ; and to hydrogen absorption at $\lambda > 12\mu$ (Gillett et al. 1969). We have smoothed

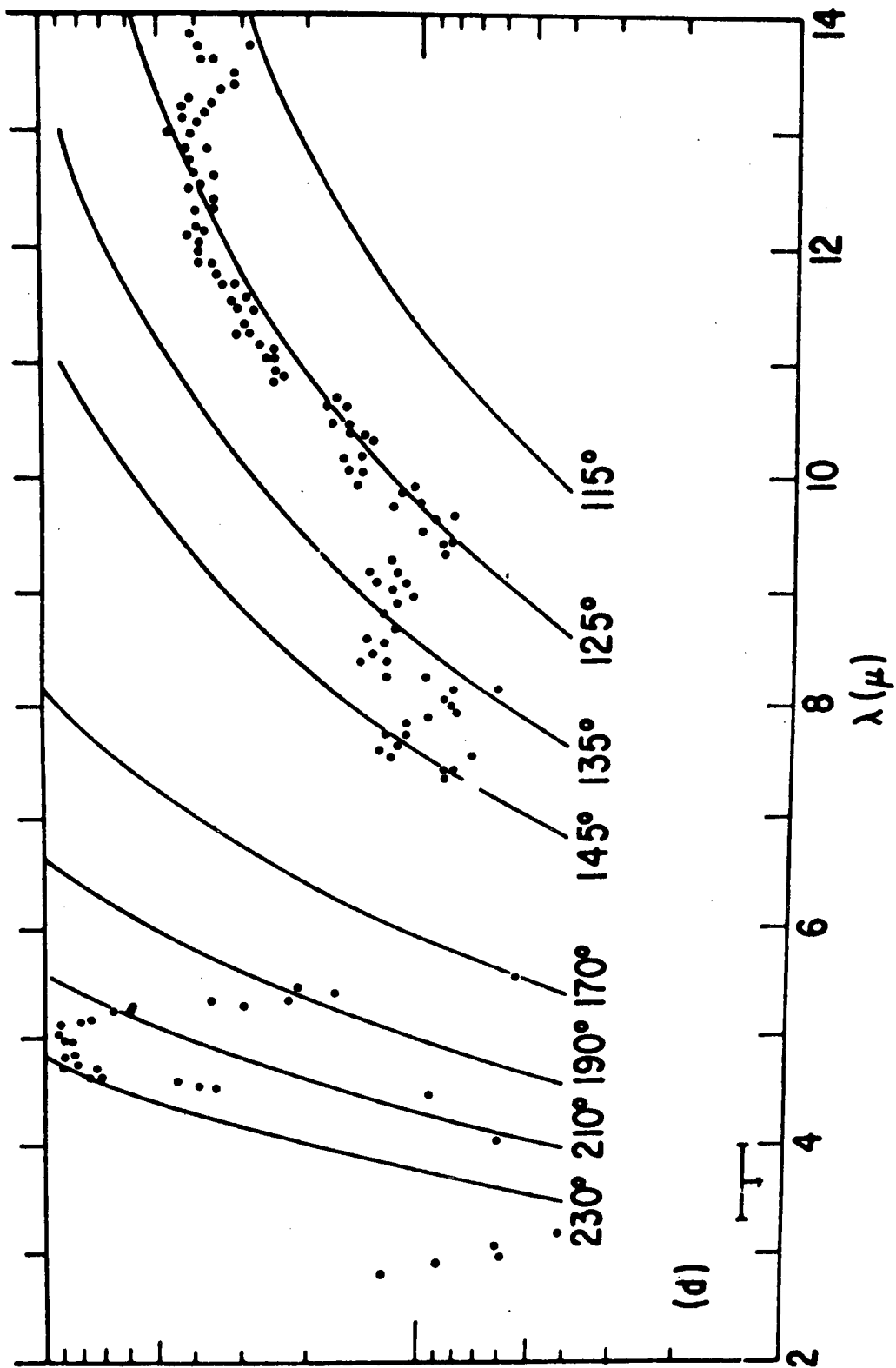


Figure 1. Observed Jovian infrared emission spectrum (after Gillett et al., 1969).

the spectrum by eye and read off the emission temperature at a number of wavelengths in each of these spectral regions. The uncertainty in reading off the temperatures may be as large as 2K. The observed emission temperatures are shown in Table 3. Observations in the CH₄ and H₂ bands are used to determine the temperature profile; observations in the NH₃ bands are used to determine the ammonia profile.

The emission spectrum of Jupiter in the vicinity of the 1.25-cm ammonia band at microwave wavelengths has been observed by Law and Staelin (1968) and Wrixon et al. (1971). The measurements of Law and Staelin cover five wavelengths between 25.4 and 19.0 GHz; those of Wrixon et al. cover eight wavelengths between 20.5 and 35.5 GHz. Additional observations at individual wavelengths within this region have been obtained by Kellerman (1970) at 15.8 GHz, Tolbert (1966) and Kalaghan and Wulfsberg (1968) at 34.9 GHz and Thornton and Welch (1963) at 36 GHz. The measured brightness temperature and their associated error flags are plotted in Figure 2, after Wrixon et al. (1971). As can be seen, there is quite a bit of uncertainty in the shape of the spectrum. We have attempted to draw a smooth curve by eye through the data on the high frequency side of the absorption band, giving more weight to the Wrixon et al. brightness temperatures because of their smaller error bars. Temperatures at three frequencies were then read off, to be used, along with the infrared NH₃ band observations, in the inversion for the ammonia profile. These microwave temperatures are shown in Table 4.

E. Results

Temperature.- The entire concept of remote probing by measuring the emission spectrum is based upon the fact that the observation radiation originates in different parts of the atmosphere, depending upon the absorption coefficient, and hence, the wavelength of the radiation. This can be seen from Figure 3, which is a plot of weighting functions, $d\tau/dz$, for the CH₄ and H₂ wavelengths used in this study. The weighting functions are proportional to the weights of equation (7) and indicate where in the atmosphere the radiation at each wavelength originates. These weighting functions are for an atmosphere consisting of the following volumetric fractions: H₂ = 0.67, He = 0.33, CH₄ = 4.7×10^{-4} . As in all the computations discussed in this paper, a vertical spacing of 2 km is used in the numerical integrations, and the zero reference level for altitude is taken to be the pressure level 5 atm.

Figure 3 indicates that at these wavelengths and for this composition, information is received on the temperature profile in the height range 25 to 100 km (if we assume that no information is received for altitudes below the altitude of the half-peak value of the lowest weighting function, or for altitudes above the altitude of the half-peak value of the highest weighting function). The hydrogen band weighting functions are narrower than the methane weighting functions due to the second power dependence of

TABLE 3

OBSERVED JOVIAN EMISSION TEMPERATURES (T_E) FOR
THE INFRARED BANDS OF CH_4 , H_2 , AND NH_3

(From Figure 1)

Absorption Band	Wavenumber (cm^{-1})	Wavelength (μ)	T_E (K)
CH_4	1160	8.6	138
	1200	8.3	138
	1220	8.2	138
	1240	8.1	139
	1260	7.9	141
	1280	7.8	145
H_2	715	14.0	120
	800	12.5	125
NH_3	862	11.6	127
	937	10.7	125
	1037	9.6	125
	1785	5.6	170
	1850	5.4	190

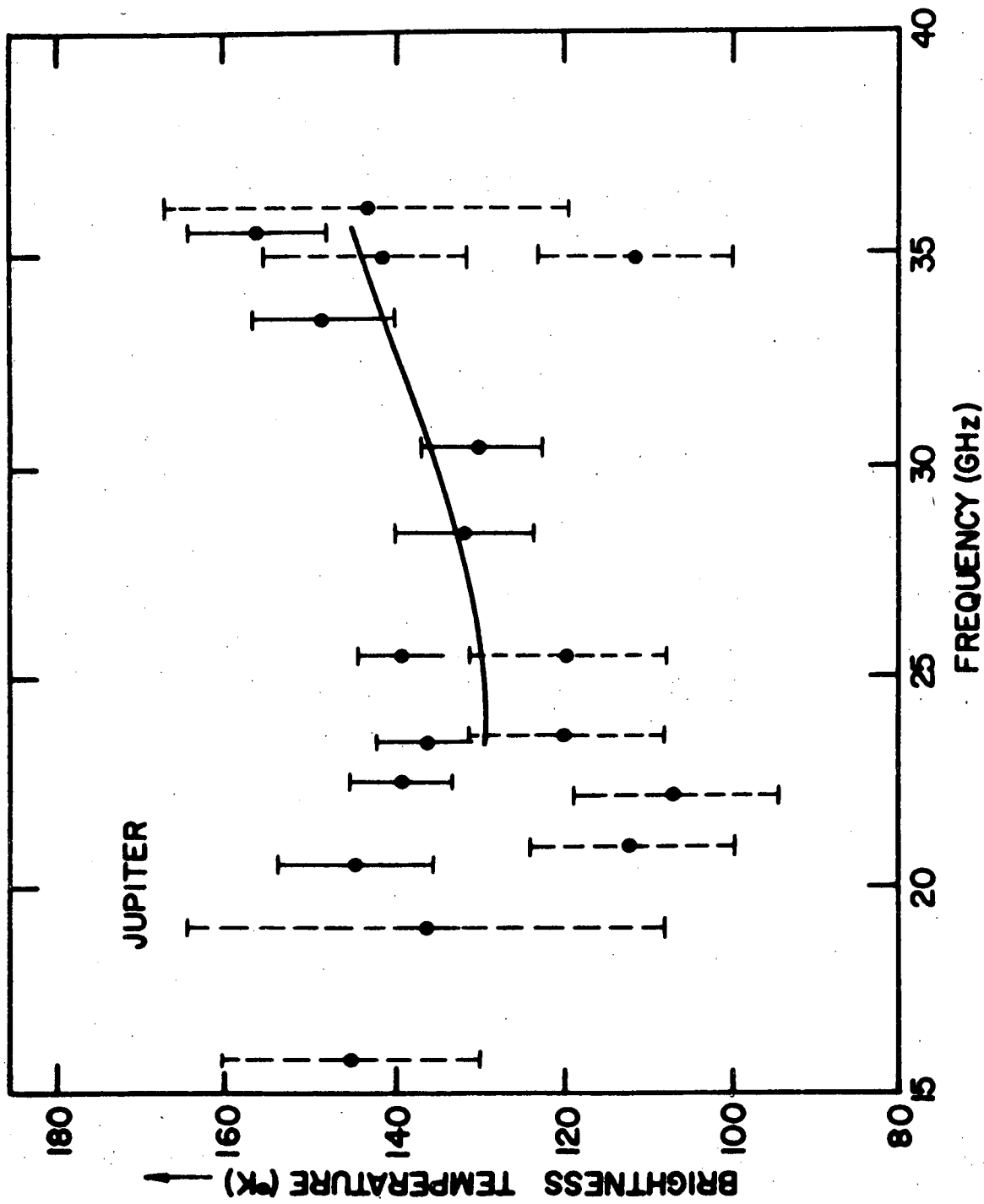


Figure 2. Observed Jovian microwave emission spectrum in the region of the 1.25-cm ammonia band. Error flags with solid lines are observations of Wrixon et al. (1971); error flags with dashed lines are observations of Law and Staelin (1968) and others. Curve through observations on high frequency side represents smoothing of the observations to derive brightness temperatures for use in the inversion procedure.

TABLE 4

OBSERVED JOVIAN BRIGHTNESS TEMPERATURES, T_B ,
FOR THE NH_3 MICROWAVE BAND

(From Figure 2)

Frequency (GHz)	Wavelength (cm)	T_B (K)
35	0.86	145
30	1.0	135
24	1.2	130

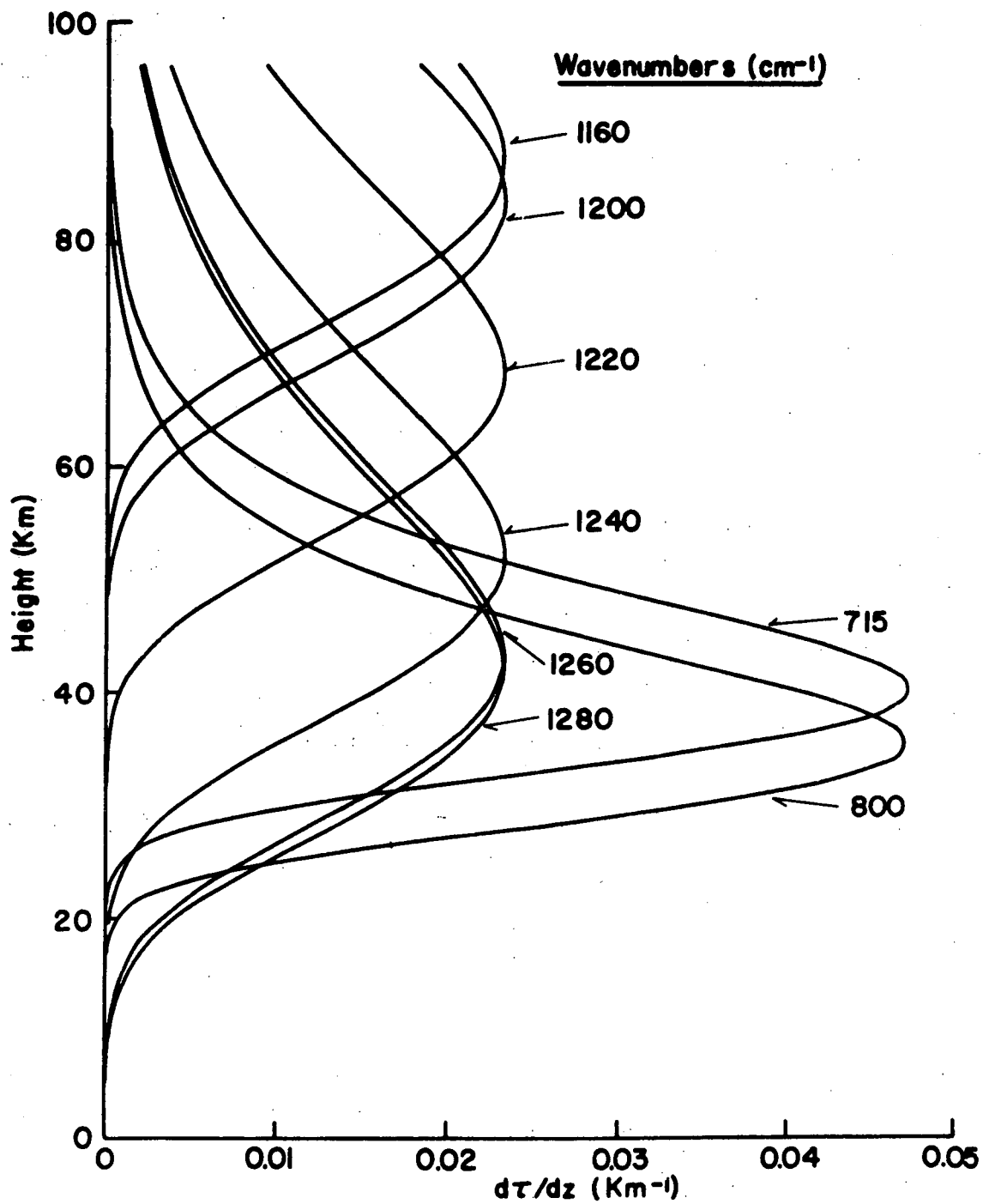


Figure 3. Weighting functions for the infrared absorption bands of CH₄ and H₂.

the hydrogen absorption coefficient on the hydrogen density. It is of interest to note that, for this atmospheric model, radiances in the two hydrogen wavenumbers and in the 1160 and 1200 cm^{-1} methane wavenumbers provide information on the atmospheric temperature in approximately the same altitude region.

We have computed the temperature profiles for several atmospheric composition models, covering the range of present uncertainties in the hydrogen and methane amounts, as discussed in Section B. The hydrogen, helium, and methane fractional volumes for these models are summarized in Table 5. In all calculations, the temperature profile was extended adiabatically from the lowest point at which information is received from the temperature inversion to the reference pressure of 5 atm.

Temperature profiles for the first set of experiments, in which the H_2 fractional volume is assumed to be 0.67, are shown as curves (a) and (b) in Figure 4. The temperature profile for a CH_4 fractional volume of 3.1×10^{-4} is almost identical with that for a CH_4 fractional volume of 4.7×10^{-4} , and, hence, is not shown. The differences in the temperature profiles are due to a slight shift upwards of the CH_4 weighting functions with respect to the H_2 weighting functions with the higher CH_4 amount. Basically, however, the profiles are similar, indicating that the derived temperature profile is not particularly sensitive to the present uncertainty in CH_4 amount. The temperature profile is characterized by a definite tropopause and stratospheric region similar to that in the earth's atmosphere. Gillett et al. (1969), interpreting their observed spectrum on the basis of a semiquantitative analysis, deduced the shape of the temperature profile shown in Figure 4 and suggested that solar heating in the 3020 cm^{-1} CH_4 band is the cause of the temperature increase above the tropopause. Radiative equilibrium temperature calculations, including absorption of solar energy in this band, have reproduced this structure (Hogan et al., 1969). Thus, it appears reasonable to conclude that the stratospheric temperature structure shown in Figure 4 is indeed real and is due to CH_4 absorption of solar radiation.

The RMS percentage difference between radiances computed from the derived temperature profiles and the observed radiances is 16 to 17 percent. One of the reasons for these differences is the relatively large differences in emission temperatures observed in the H_2 band and those observed in the 1160 to 1200 cm^{-1} region of the CH_4 band. As indicated earlier, the radiances at these wavenumbers refer to approximately the same atmospheric region, and hence, they should yield the same emission temperature. The fact that they do not suggests that they are inconsistent. The iterative inversion scheme handles this inconsistency by objectively weighting each of the radiances so that the resulting temperature is based upon a suitable average of the observations. It should also be pointed out that in the region of the methane band at 8μ , and at the temperatures of the Jovian atmosphere, a one degree change in atmospheric temperature is

TABLE 5

ATMOSPHERIC COMPOSITION (FRACTIONAL VOLUME) MODELS USED FOR
CALCULATIONS OF TEMPERATURE PROFILE

Experiment No.	H ₂	He	CH ₄
1	0.67	0.33	4.7 x 10 ⁻⁴
2	0.67	0.33	3.1 x 10 ⁻⁴
3	0.67	0.33	1.6 x 10 ⁻³
4	1.00	0	7.0 x 10 ⁻⁴
5	1.00	0	4.7 x 10 ⁻⁴
6	1.00	0	2.3 x 10 ⁻³

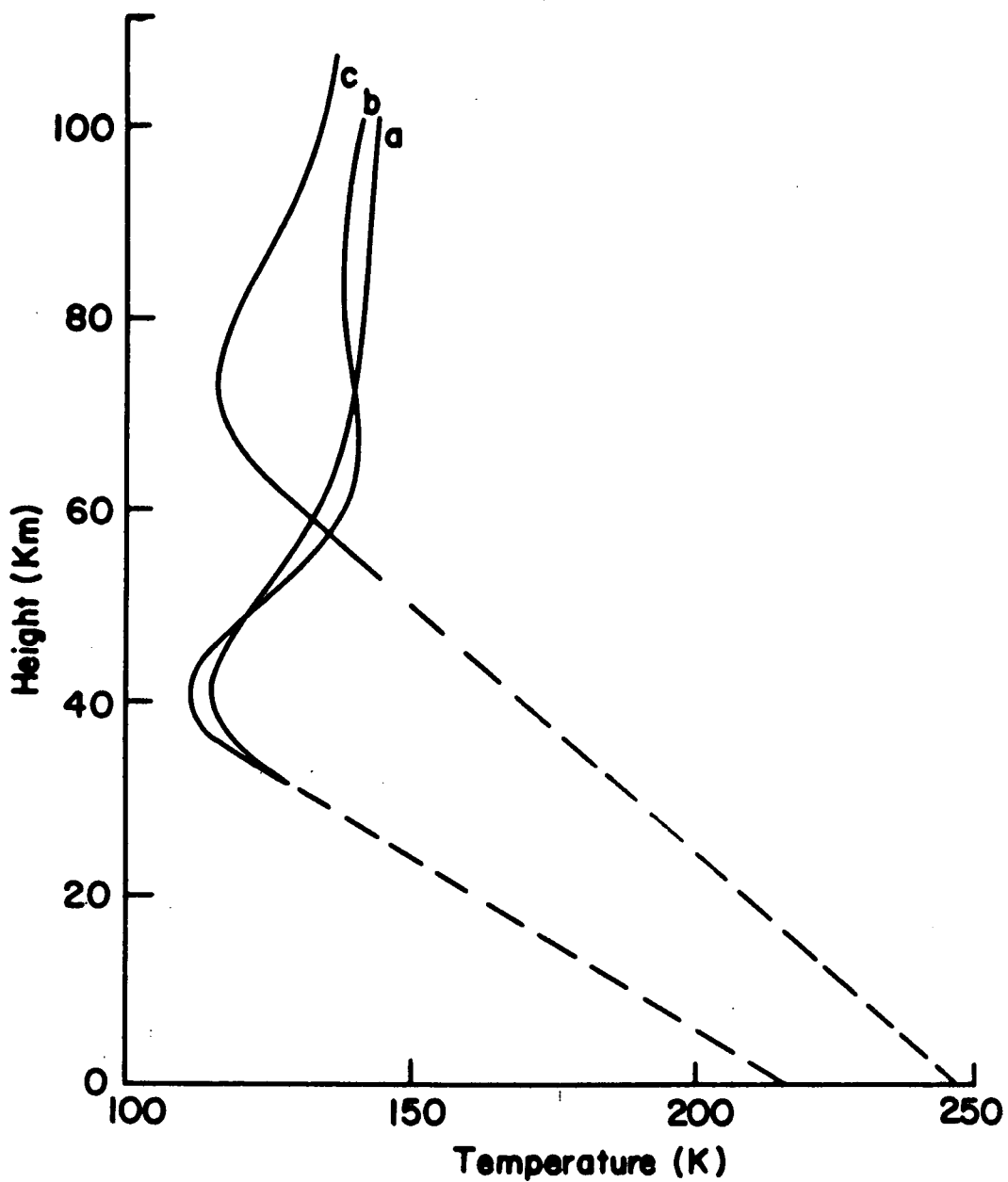


Figure 4. Inferred temperature profiles: (a) Experiment 2, (b) Experiment 3, (c) Experiment 5. Dashed lines represent adiabatic extensions of inferred temperature profiles to a pressure level of 5 atmospheres, which serves as the zero reference for the altitude scale.

equivalent to a 10 percent change in radiance. Thus, 20 percent RMS differences between observed and computed radiances in the methane band represent temperature differences of only 2K.

Temperature profiles for the second set of model atmospheres ($H_2 = 1.0$) were almost identical and, hence, only one of this set is plotted in Figure 4, as curve (c). The main effect of a pure H_2 atmosphere is an increase in the scale height which leads to an increase in the altitudes of and a broadening of the weighting functions. The derived temperature profiles for these cases are characterized by much higher tropopause. Again, there is little difference in temperature profile with varying amounts of CH_4 . RMS percentage differences between radiances computed with these temperature profiles and the observed radiances are in the range 15 to 17 percent.

Ammonia. - Making use of the derived temperature profiles, we have computed ammonia profiles for the same model atmospheres of Table 5. Ammonia weighting functions for the initial guess ammonia profile are shown in Figure 5. This ammonia profile is characterized by a total abundance above the 5 atm level of 1.3×10^3 atm cm and a scale height of 1.6 km. The chosen guess scale height is intended to simulate an NH_3 saturation condition. The hydrogen volume fraction is 0.67. The NH_3 weighting functions are narrower than the CH_4 or H_2 weighting functions due to the small NH_3 scale height.

Ammonia profiles for the first set of experiments ($H_2 = 0.67$) are all similar; hence, only one is plotted in Figure 6, that for experiment 2. The final NH_3 weighting functions for this ammonia profile are shown in Figure 7. It is assumed that no information is obtained on the NH_3 profile below the peak of the lowest weighting function or above the peak of the highest weighting function. The quantity plotted in Figure 6 is the NH_3 abundance as a function of altitude. NH_3 partial pressures, determined from the abundance profile, were compared to saturation vapor pressures for NH_3 . The region where NH_3 saturation was found is indicated in the graph. Thus, at an altitude of about 30 km, an ammonia ice crystal cloud would presumably be present with a base temperature of 142K and top temperature of 130K.

For clarity, in the graph of the NH_3 weighting functions associated with the NH_3 profile, only one weighting function from each of the three NH_3 absorption bands is plotted. The multiple peaks of the final weighting functions is due to the unsmooth character of the final NH_3 profile. The unsmooth final profile may, in turn, be due to inconsistencies in the observed radiances in the three NH_3 absorption bands.

Ammonia profiles for the second set of experiments ($H_2 = 1.00$) are also almost identical; hence, only the computed profile for experiment 5 is shown (Figure 8). The shape of the profile is similar to that of the $H_2 = 0.67$ case. However, the ammonia is now at a higher altitude and its

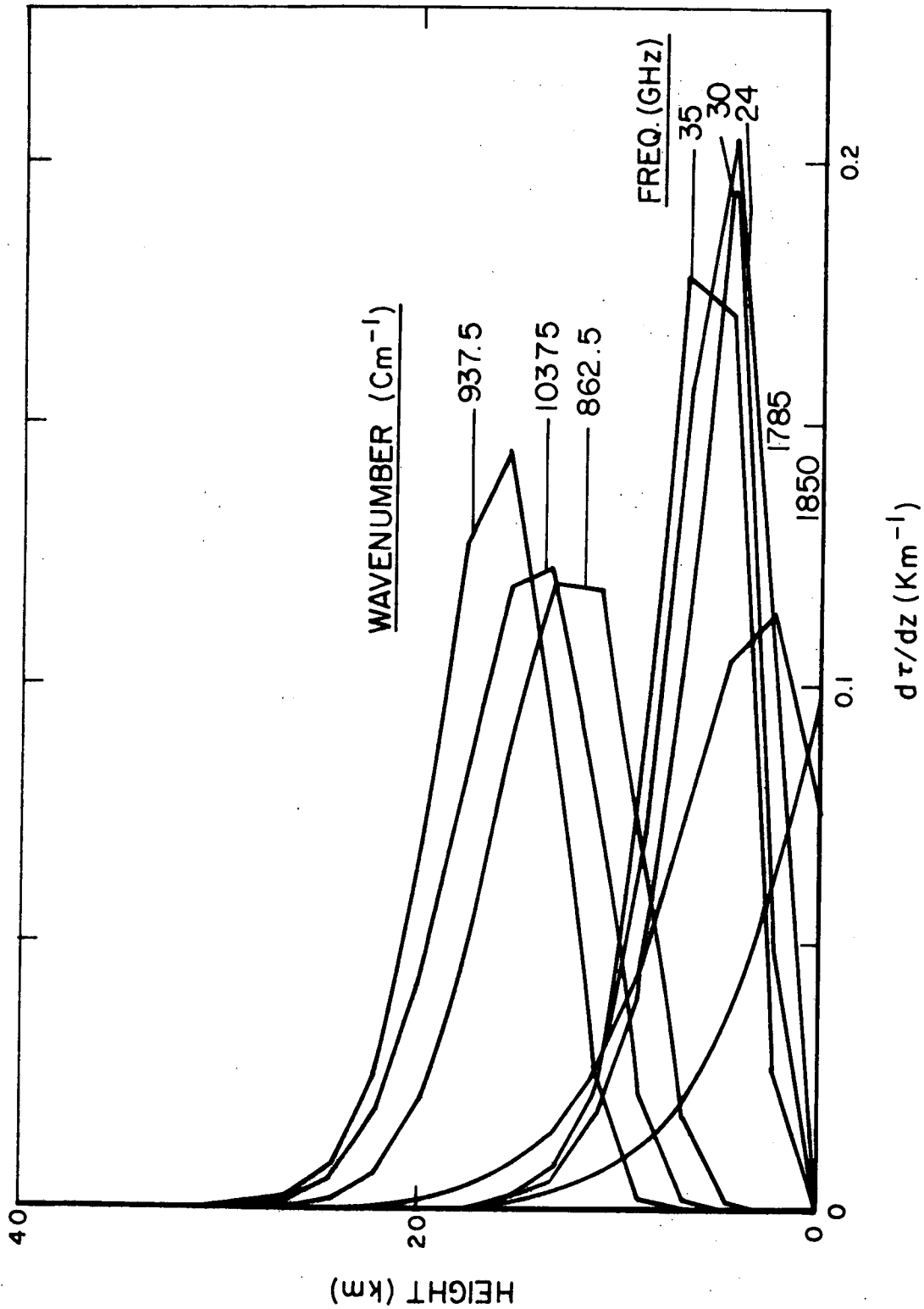


Figure 5. NH_3 weighting functions for the initial "guess" NH_3 profile characterized by a total abundance of 1.3×10^3 atm-cm and a scale height of 1.6 km.

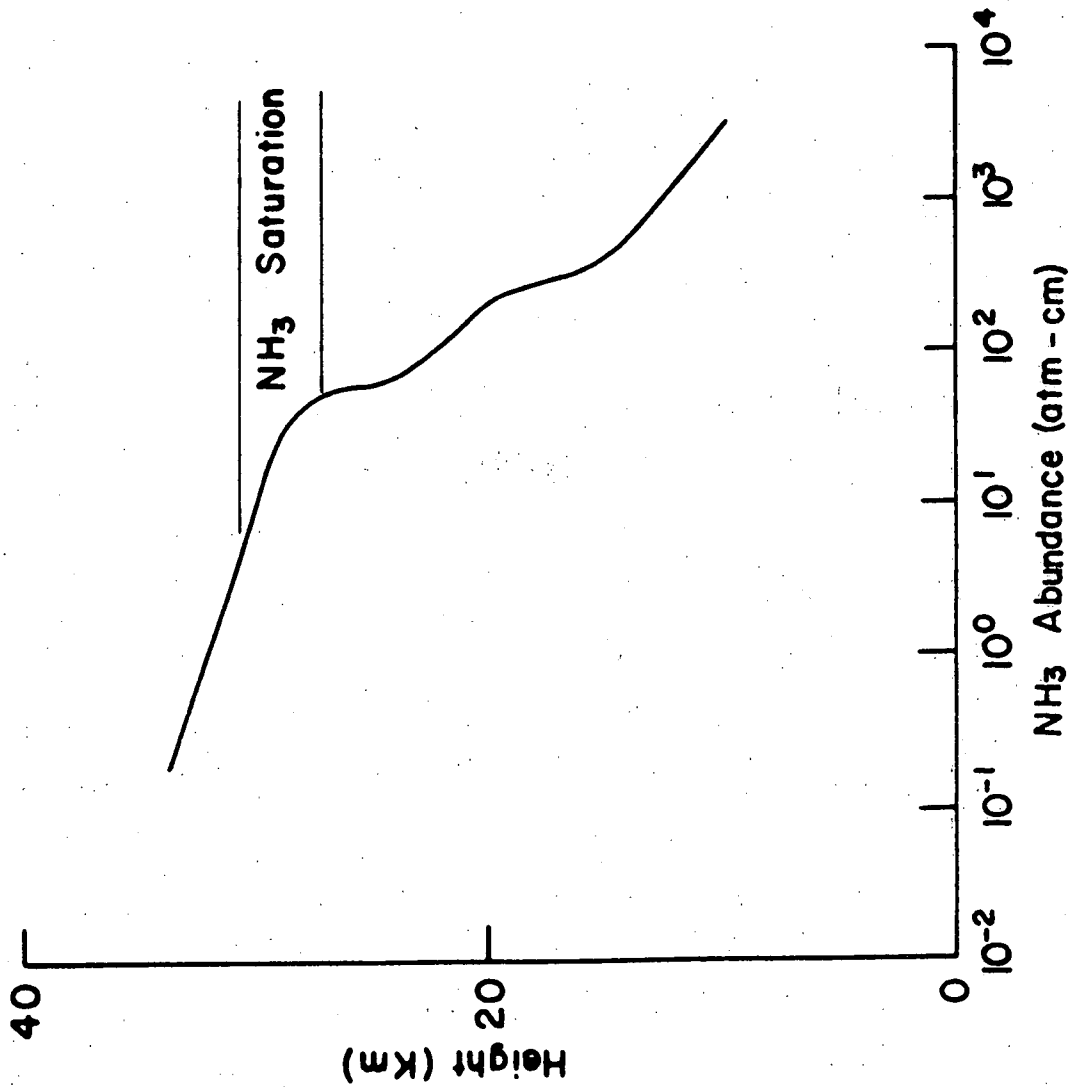


Figure 6. Inferred NH_3 abundance profile for an H_2 fractional volume of 0.67 (Experiment 2).

C

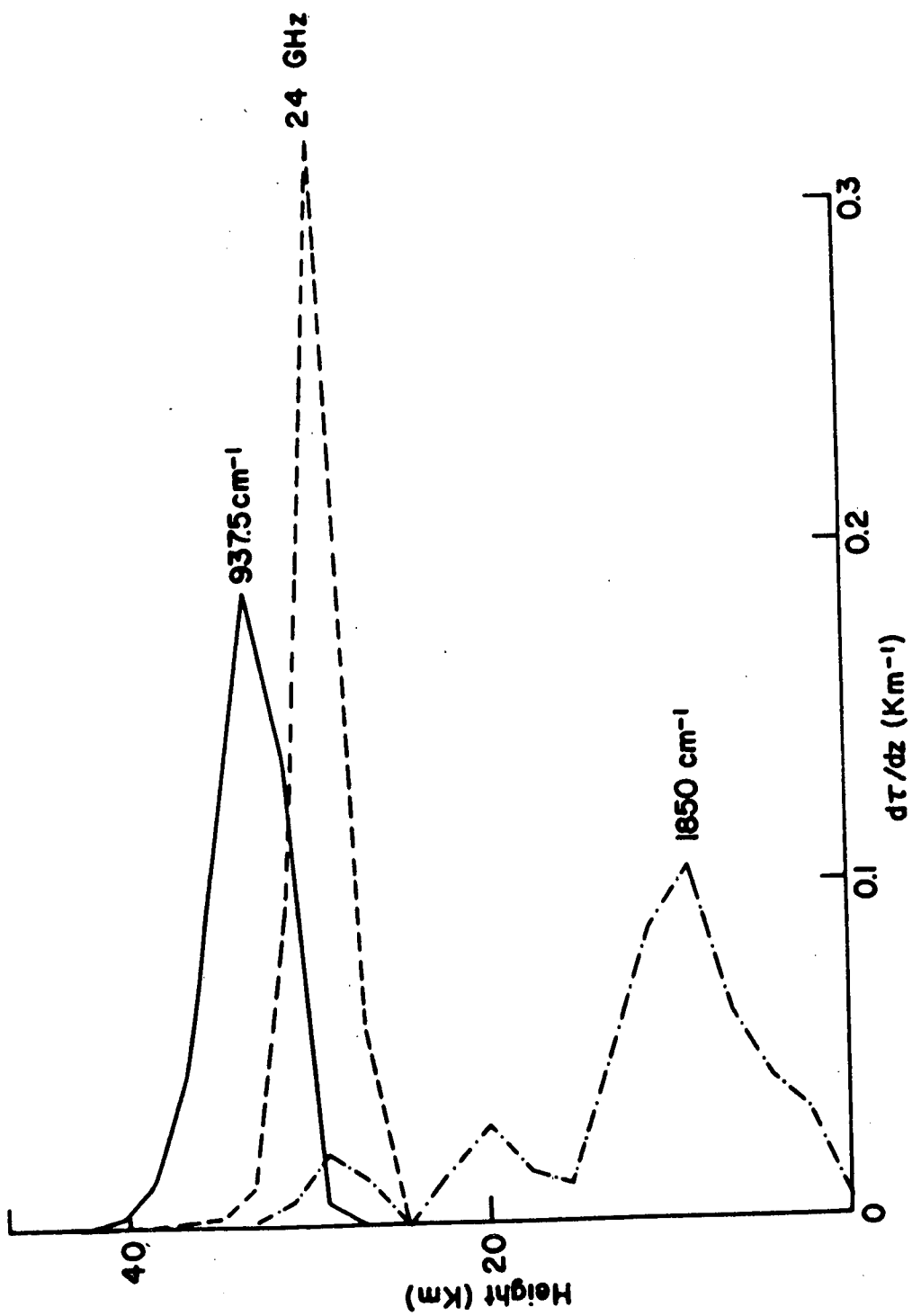


Figure 7. NH₃ weighting functions for inferred NH₃ abundance profile of Figure 6.

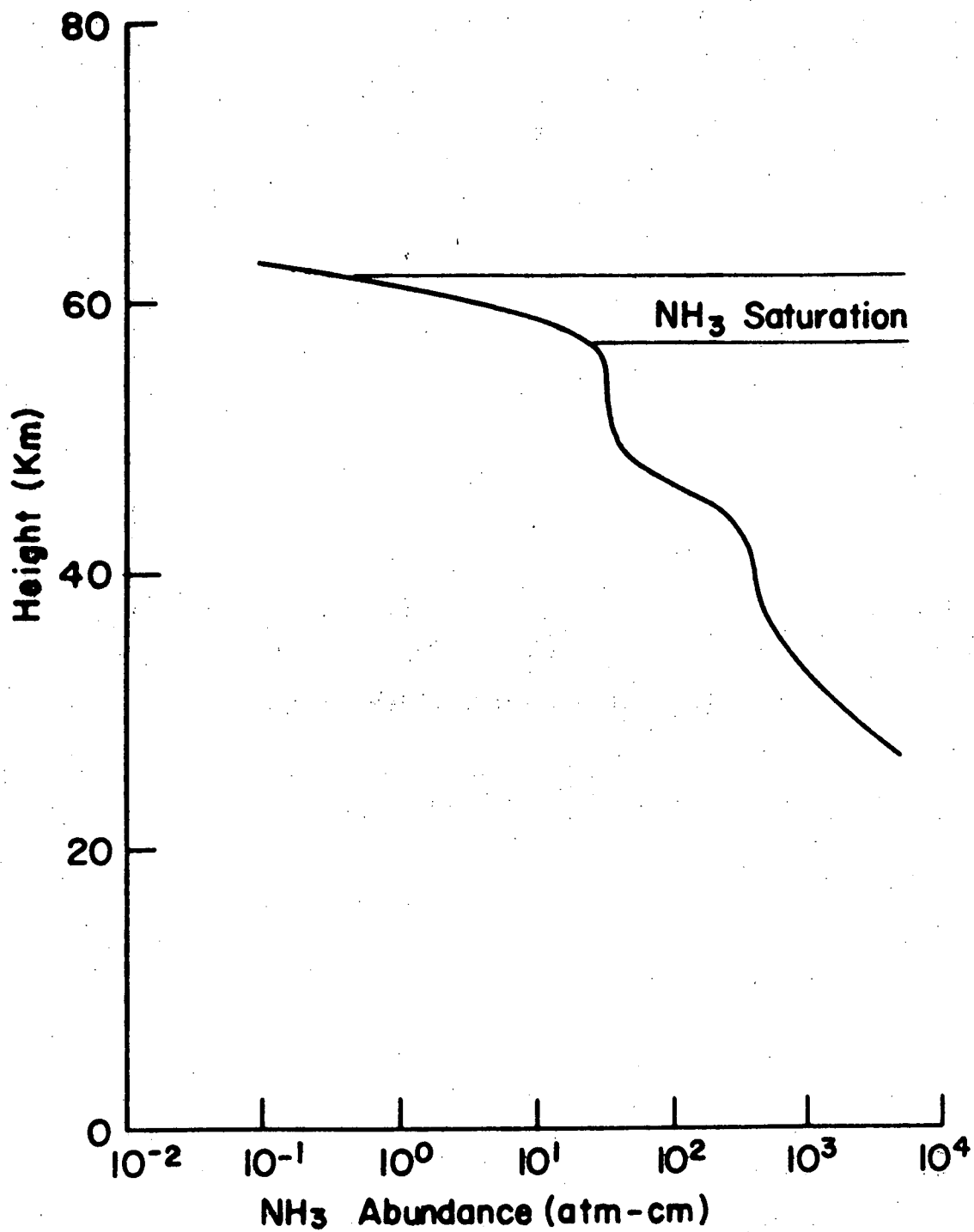


Figure 8. Inferred NH₃ abundance profile for an H₂ fractional volume of 1.0 (Experiment 5).

scale height is greater. Both of these differences are ultimately due to the greater scale heights of the $H_2 = 1.00$ atmosphere. A saturated layer is also found for this set of experiments at an altitude of about 60 km, with a base temperature of 137K and top temperature of 129K. RMS percentage differences between the radiances computed with the final NH_3 profile and the observed radiances are ≈ 6 percent for this set; for the first set, the RMS percentage differences are ≈ 7 percent.

The derived NH_3 abundances may be compared to some of the values found in the literature. With the use of a reflecting layer hypothesis, total abundances of 7×10^2 (Kuiper, 1952) and 1.2×10^3 cm atm (Owen, 1969) have been obtained from the 6470\AA observations. Our maximum value of abundance is of the order of 4×10^3 atm cm. This would be in rough agreement with Owen's value if the reflecting level is close to the level of our maximum value of abundance. The model builders suggest NH_3 cloud base temperatures of 150K (Danielson and Tomasko, 1971) and 160K (Owen, 1969). NH_3 cloud base temperatures derived from the present analyses are in the vicinity of 140K. The present analysis supports Danielson and Tomasko's suggestion of an upper, thin NH_3 ice crystal cloud in the Jovian atmosphere.

F. Conclusions

Inversion techniques for temperature and atmospheric composition, originally developed for analyzing meteorological satellite observations of the earth's infrared emission spectrum, have been successfully applied to earth based observations of the Jovian infrared and microwave emission spectrum. Temperature and ammonia profiles for the Jovian atmosphere have been derived. The derived Jovian temperature profile is characterized by a tropopause region with a temperature of 115K located in the pressure range 0.3 to 0.6 atm and a stratospheric region in which the temperature increases with altitude. The actual tropopause temperature may be somewhat lower than 115K since the temperatures derived from the inversion represent essentially vertically averaged temperatures, the vertical resolution being related to the widths of the weighting functions. The derived ammonia profile is characterized by a total abundance of $\approx 4 \times 10^3$ atm-cm above the pressure level 2 atm, a rapid decrease of NH_3 with altitude (compared to the rate of decrease of total atmospheric density), and a relatively thin (≈ 5 km) saturated layer at a base temperature of ≈ 140 K.

There are a number of uncertainties in the present inversions. These include the errors in the radiance observations (particularly in the microwave region) and uncertainties in the transmittance models used (particularly for the 6.1μ band of NH_3). However, the results are consistent with present ideas on the Jovian atmosphere and suggest that inversion of the Jovian emission spectrum is a powerful method for sounding the Jovian atmosphere. With a minimum of assumptions, one can derive temperature and ammonia profiles directly from the radiance observations. Improved inversions can be obtained from fly-by or orbiter observations of the Jovian infrared and microwave spectrum, or from more accurate earth based observations, together with more accurate transmittance models.

REFERENCES

- Anderson, R.C., Pipes, J.G., Broadfoot, A.L., and Wallace, L., *J. Atmos. Sci.* 26, 874 (1969).
- Ben Reuven, A., *Phys. Rev.* 145, 7 (1966).
- Bleaney, B., and Loubser, J., *Proc. Phys. Soc.* 77, 418 (1950).
- Chahine, M.T., *J. Atmos. Sci.* 27, 960 (1970).
- Danielson, R.E., and Tomasko, M.G., *J. Atmos. Sci.* 26, 889 (1969).
- Gille, J.C., and Lee, T.H., *J. Atmos. Sci.* 26, 932 (1969).
- Gillett, F.C., Low, F.J., and Stein, W., *Ap. J.* 157, 925 (1969).
- Hogan, J., Rasool, S.I., and Encrenaz, T., *J. Atmos. Sci.* 26, 898 (1969).
- Kalaghan, P.M., and Wulfsberg, K.N., *Ap. J.* 154, 771 (1968).
- Kellermann, K.I., *Radio Sci.* 5, 487 (1970).
- Kuiper, G.P., Atmospheres of the Earth and Planets, (Chicago: University of Chicago Press) (1952).
- Law, S.E., and Staelin, D.H., *Ap. J.* 154, 1077 (1968).
- McClatchey, R.A., Fenn, R., Selby, J., Garing, J., and Voltz, R., Environmental Research Papers No. 331, Air Force Cambridge Research Laboratories, 85 pp. (1970).
- McElroy, M., *J. Atmos. Sci.* 26, 798 (1969).
- Owen, T., *Icarus* 10, 355 (1969).
- Ohring, G., *Quart. Rept. No. 1*, NASA Contract NASW-2221, GCA Corporation, Bedford, Mass., 34 pp. (1971).
- Smith, W., *Appl. Optics* 9, 1993 (1970).
- Taylor, F.W., *J. Atmos. Sci.* 29, 950 (1972).
- Tolbert, C.W., *A.J.* 71, 30 (1966).
- Townes, C., and Schzwlow, A., Microwave Spectroscopy (New York: McGraw-Hill Book Co.) (1955).
- Thornton, D.D., and Welch, W.J., *Icarus* 2, 228 (1963).
- Trafton, L.M., *Ap. J.* 147, 765 (1967).
- Trafton, L.M., and Munch, G., *J. Atmos. Sci.* 26, 813 (1969).
- Wildey, R.L., and Trafton, L.J., *Ap. J. (Supp. Ser.)* 23, 1 (1971).
- Wrixon, G.T., Welch, W.J., and Thornton, D.D., *Ap. J.* 169, 171 (1971).

SECTION III

A TECHNIQUE TO DEDUCE THE MARTIAN ATMOSPHERIC TEMPERATURE AND WATER VAPOR PROFILES FROM ORBITER OBSERVATIONS OF THE PLANET'S IR LIMB RADIANCE PROFILE

A. Introduction

The inference of atmospheric temperature and constituent profiles from measurements of the spectral distribution of the emitted thermal radiation from a planetary atmosphere has received a good deal of attention recently. Such experiments have already been successfully flown in the Earth orbiting NIMBUS satellites (see, for example, Conrath et al., 1970), have been flown on the Mariner 9 flight to Mars (Hanel et al., 1972), and will be flown on future flights to Mars and Venus. Another technique, based upon scanning the limb of the planet rather than scanning in wavelength, can also provide valuable information on the vertical profiles of temperature and constituents of a planetary atmosphere. This concept is just beginning to receive attention (Gille and House, 1971) and will be tested on the NIMBUS F meteorological satellite. This technique has certain advantages over the spectral scan, and can be used to complement spectral scans.

The basic geometry of the limb, or horizon, radiance observation is shown in Figure 1. A high angular resolution (~ 0.1 degrees for orbital altitude of 10^3 km) radiometer on a planetary orbiter intercepts radiation emanating from an atmospheric path that is tangent to the planetary surface at height h , which is termed the tangent height. In the figure, R represents altitude. The wavelength interval to which the radiometer is sensitive is determined by the nature of the experiment. If the temperature profile is the object of the experiment, the wavelength interval will lie in an atmospheric absorption band of a constituent whose distribution is known - e.g., the 15μ CO_2 band would be a good choice for Earth, and possibly, Mars and Venus. If the water vapor profile is the object of the measurement, then an infrared water vapor band would be selected. The radiation received by the instrument is a function of the distribution of temperature and absorbing gas along the ray path. If the distribution of absorbing gas is known, the temperature above the tangent height can be inferred from the radiance observations. If the temperature distribution is known, we can infer the distribution of an absorbing gas. By scanning in tangent height from top to base of the atmosphere, it is thus possible to infer the vertical temperature structure or vertical distribution of absorbing gas. The radiance versus tangent height curve obtained through such a scan is called a horizon radiance profile or limb radiance profile. The geometry of the horizon radiance observation technique insures that one is receiving information on the temperature, for example, from the atmosphere above a particular level - the tangent height. It will be shown below that for a gas with constant mixing ratio - such as CO_2 in the

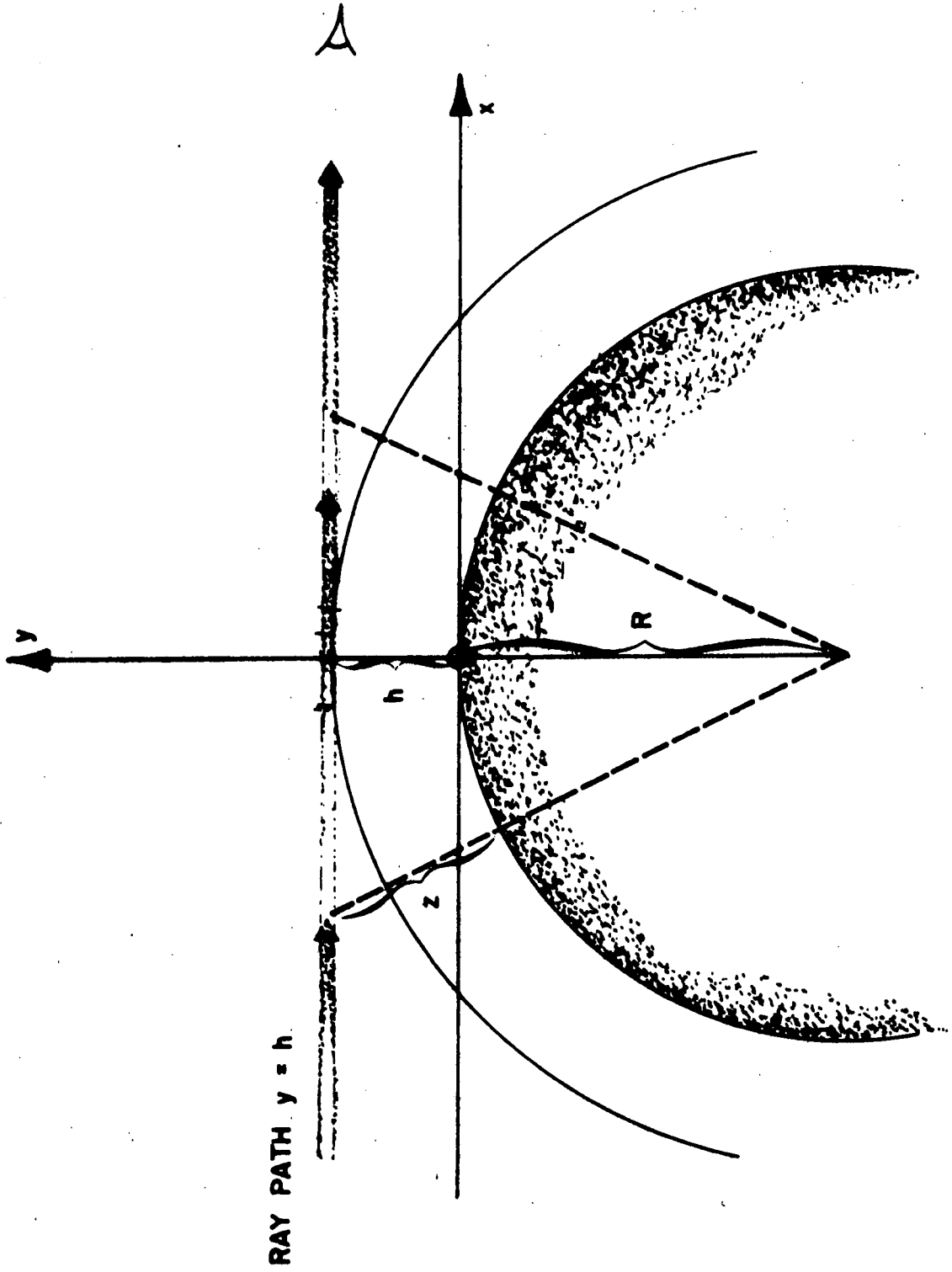


Figure 1. Limb Viewing Geometry.

atmosphere of Earth and probably in the atmospheres of Mars and Venus (at least to great heights) - the weighting functions for the horizon radiance observation are sharply peaked at the tangent height. This means that not only is the vertical slice of atmosphere under view limited at its lower bound by the tangent height being observed, but its upper bound is also effectively limited by the shape of the weighting function. In other words, for a particular tangent height h , most of the radiation comes from a rather narrow vertical interval between h and $h + \Delta Z$. Hence, the mean temperature of this interval could easily be inferred by an 'instant inversion' technique.

Below we develop the technique for two infrared transmission models: the Goody random model, and the transmission models used by Bartko and Hanel (1968) for calculations of temperature in the upper atmosphere of Venus. We then compute weighting functions for the atmosphere of Mars using the Goody random model.

B. Theory

The intensity of radiation received by an infrared radiometer with narrow field of view whose line of sight is tangent to the planetary atmosphere at the tangent height, h of Figure 1, is given by

$$I = \int_{-\infty}^{\infty} B \frac{\partial \tau}{\partial x} dx = \int_0^{\infty} B \frac{\partial \tau}{\partial x} dx + \int_{-\infty}^0 B \frac{\partial \tau}{\partial x} dx \quad (1)$$

where B is the Planck intensity integrated over the spectral interval of the radiometer, and τ is the spectral transmittance of the atmosphere from the point x to the radiometer. From the geometry, the following relationship between x and height z exists

$$(R + h)^2 + x^2 = (R + z)^2 \quad (2)$$

The terms h^2 and z^2 can be neglected in comparison with the other terms - since we are interested in the lower part of the atmosphere ($Z < 100$ km) - so that

$$x = \sqrt{2R(z - h)} \quad (3)$$

and

$$dx = \left(\frac{R}{2} \right)^{1/2} \frac{1}{(z-h)^{1/2}} dz \quad (4)$$

Thus Equation (1) can also be written as

$$I = \int_h^{\infty} B \frac{\partial \tau}{\partial z} dz + \int_{-\infty}^h B \frac{\partial \tau}{\partial z} dz \quad (5)$$

Expressions will be derived first for the weighting functions

$$\frac{\partial \tau}{\partial z}$$

which determine where in the atmosphere the radiation received by the sensor originates. We assume that the observations are made in a CO₂ band for purposes of temperature inferences.

Goody Random Model.- If it is assumed that the transmittance is given by the Goody random model, then

$$\tau = \exp \left[- \frac{k\bar{m}}{\delta} \left(1 + \frac{k\bar{m}}{\pi\bar{\alpha}} \right)^{-1/2} \right] \quad (6)$$

where k is the mean line intensity, δ is the mean line spacing, \bar{m} is the effective amount of absorbing gas in $g\text{ cm}^{-2}$ along the path, and $\bar{\alpha}$ is the effective half-width along the path. For the Martian and Venusian CO₂ amounts and pressures, and the long paths of concern here, $k\bar{m}/\pi\bar{\alpha}$ is much greater than unity. Thus, Equation (6) can be written as

$$\tau = \exp \left[- \left(\frac{k\pi\bar{m}\bar{\alpha}}{\delta^2} \right)^{1/2} \right] \quad (7)$$

Following Rodgers and Walshaw (1966), the effective absorber amount and half-width are

$$\bar{m} = \int \Phi(\theta) dm \quad (8)$$

and

$$\bar{\alpha} = \frac{\int \alpha dm}{\int dm} \quad (9)$$

where $\Phi(\theta)$ is a correction for the effect of temperature on the line intensities and is given by

$$\log_e \Phi(\theta) = a(\theta - 260) + b(\theta - 260)^2, \quad (10)$$

where θ is temperature and a and b are constants for the band. For the present purpose of determining the CO_2 transmittances, an isothermal atmosphere is assumed so that

$$\bar{m} \bar{\alpha} = \Phi(\theta) \int \alpha dm \quad (11)$$

Since

$$\alpha = \alpha_s \left(\frac{p}{p_s} \right) \left(\frac{\theta}{\theta_s} \right)^{1/2} \quad (12)$$

where p is pressure and the subscript s refers to standard temperature and pressure, and $dm = \rho_{\text{CO}_2}$

$$dx = \rho_c \left(\frac{R}{2}\right)^{1/2} \frac{1}{(z-h)^{1/2}} dz, \quad (13)$$

where ρ_{CO_2} is the carbon dioxide density, ρ is the atmospheric density, and c is the CO_2 mass fraction, Equation (11) can be written as

$$\bar{m} \bar{\alpha} = \phi(\theta) \alpha_s \left(\frac{1}{p_s}\right) \left(\frac{\theta_s}{\theta}\right)^{1/2} \left(\frac{R}{2}\right)^{1/2} c \int_z^{\infty} p \rho \frac{dz}{(z-h)^{1/2}} \quad (14)$$

For an isothermal atmosphere both pressure and density have the same scale height H . Thus, Equation (14) becomes

$$\bar{m} \bar{\alpha} = \phi(\theta) \alpha_s \left(\frac{p_o}{p_s}\right) \left(\frac{\theta_s}{\theta}\right)^{1/2} \left(\frac{R}{2}\right)^{1/2} c \rho_o \int_z^{\infty} e^{-z/H} \frac{dz}{\sqrt{z-h}} \quad (15)$$

where the subscript o refers to surface values on the planet.

With the substitution,

$$t^2 = \frac{2(z-h)}{H}$$

the integral in Equation (15) becomes

$$e^{-2h/H} (2H)^{1/2} \int_0^{\infty} e^{-t^2} dt \sqrt{\frac{2(z-h)}{H}} \quad (16)$$

The integral in Equation (16) is equal to $\frac{\sqrt{\pi}}{2} [1 - \text{erf } \alpha]$, where erf is the error function, and $\alpha = \sqrt{2(z-h)}/H$. Thus

$$\bar{m} \bar{\alpha} = \phi(\theta) \alpha_s \left(\frac{p_o}{p_s} \right) \left(\frac{\theta_s}{\theta} \right)^{1/2} \frac{(\pi R H)^{1/2}}{2} c \rho_o e^{-2h/H} \left[1 \mp \operatorname{erf} \left(\frac{2(z-h)}{H} \right)^{1/2} \right] \quad (17)$$

where the negative sign in front of the error function is to be used for anterior values of z (to the right of the y axis in Figure 1) and the positive sign for posterior values of z . The expression for the transmittance from the point z to $z = \infty$ can now be written as

$$\tau(z, h) = \exp \left\{ -A e^{-h/H} \left[1 \mp \operatorname{erf} \left(\frac{2(z-h)}{H} \right)^{1/2} \right]^{1/2} \right\} \quad (18)$$

where

$$A^2 = \frac{k\pi}{\delta^2} \phi(\theta) \alpha_s \left(\frac{p_o}{p_s} \right) \left(\frac{\theta_s}{\theta} \right)^{1/2} \frac{(\pi R H)^{1/2}}{2} c \rho_o \quad (19)$$

Differentiating with respect to z yields

$$\frac{d\tau}{dz}(z, h) = \pm \frac{1}{\sqrt{2(z-h)H}} \frac{A}{\sqrt{\pi}} \exp \left[-A e^{-h/H} \left(1 \mp \operatorname{erf} \sqrt{\frac{2(z-h)}{H}} \right)^{1/2} \right] \left(1 \mp \operatorname{erf} \sqrt{\frac{2(z-h)}{H}} \right)^{-1/2} e^{-(2z-h)/H} \quad (20)$$

where the upper signs are to be used for anterior values of z and the lower signs for posterior values of z .

Bartko-Hanel transmission model.- The Bartko-Hanel (1968) transmittance for a spectral interval can be written as

$$\tau = \exp \left[- (\mu u^*)^n \right] \quad (21)$$

where m and n are constants for the spectral interval, and u^* , the effective absorber amount, is given by

$$u^* = \left(\frac{T_s}{T} \right)^{3/2} \exp \left[\gamma \left(\frac{1}{T_s} - \frac{1}{T} \right) \right] \left(\frac{p}{p_s} \right)^k u \quad (22)$$

where u is path-length of absorbing gas in units of atmo-cm of CO_2 , T_s and p_s are standard temperature and pressure, respectively, and γ is a constant for a spectral interval. Expression (22) is for a constant temperature and pressure path. We assume an isothermal atmosphere and, hence, a constant temperature for purposes of evaluating transmittances. The pressure does vary over the path and in this case expression (22) p^k is replaced by \bar{p}^k , where the bar represents an average over the atmospheric path.

$$\bar{p}^k = \int p^k du / \int du \quad (23)$$

From the definition of the path length,

$$du = \frac{\rho_{\text{CO}_2}}{\rho'_{\text{CO}_2}} dx = \frac{c\rho}{\rho'_{\text{CO}_2}} \left(\frac{R}{2} \right)^{1/2} \frac{1}{(z-h)^{1/2}} dz \quad (24)$$

where the prime represents conditions of standard temperature and pressure, and c is the CO_2 mass fraction.

The effective absorber amount can then be written as

$$u^* = f(T) p_s^{-k} \int p^k du \quad (25)$$

where

$$f(T) = \left(\frac{T_0}{T} \right)^{3/2} \exp \left[\gamma \left(\frac{1}{T_s} - \frac{1}{T} \right) \right] \quad (26)$$

or

$$u^* = B \int_z^\infty p^k \rho \frac{dz}{(z-h)^{1/2}} \quad (27)$$

where

$$B = \frac{f(T) p_s^{-k} c}{\rho_{CO_2}} \left(\frac{R}{2} \right)^{1/2} \quad (28)$$

Under the assumption of an isothermal atmosphere (for transmission calculations only), both pressure and density have the same scale height H. Thus,

$$u^* = B p_0^k \rho_0 \int_z^\infty \exp \left[-(k+1) z/H \right] \frac{dz}{(z-h)^{1/2}} \quad (29)$$

where the subscript o refers to the planet's surface.

If we let

$$t^2 = \frac{(k+1)(z-h)}{H} \quad (30)$$

the integral in (29) becomes

$$2 \left(\frac{H}{k+1} \right)^{1/2} \exp \left[-(k+1)h/H \right] \int_0^{\infty} e^{-t^2} dt \quad (31)$$

$$\sqrt{\frac{(z-h)(k+1)}{H}}$$

The integral in Equation (31) is equal to $\frac{\sqrt{\pi}}{2} (1 - \operatorname{erf} \alpha)$, where

$$\alpha = \sqrt{(z-h)(k+1)/H} \quad (32)$$

Thus,

$$u^* = B p_o^k \rho_o \left(\frac{\pi H}{k+1} \right)^{1/2} \exp \left[-(k+1)h/H \right] (1 \mp \operatorname{erf} \alpha) \quad (33)$$

where the negative sign in front of the error function is to be used for anterior values of z , and the positive sign for posterior values of z . The expression for the transmittance from the point z to $z = \infty$ along the tangent path can be written as

$$\tau = \exp \left\{ mE \exp \left[-(k+1)h/H \right] (1 \mp \operatorname{erf} \alpha) \right\}^n \quad (34)$$

where

$$E = B p_0^k \rho_0 \left(\frac{\pi H}{k+1} \right)^{1/2} \quad (35)$$

Differentiating with respect to z yields

$$\frac{d\tau}{dz}(z,h) = \pm n \left[\frac{k+1}{\pi H(z-h)} \right]^{1/2} \exp - \left\{ mE \exp - \left[(k+1)h/H \right] (1 \mp \operatorname{erf} \alpha) \right\}^n \\ \left\{ mE \exp \left[-(k+1)h/H \right] (1 \mp \operatorname{erf} \alpha) \right\}^{n-1} e^{-\alpha^2} \quad (36)$$

C. Application to the Problem of Inferring the Martian Temperature Profile

The weighting function is defined as

$$W(z,h) = \left[\frac{d\tau}{dz}(z,h) \right]_A - \left[\frac{d\tau}{dz}(z,h) \right]_P \quad (37)$$

with A and P standing for anterior and posterior, respectively.

We have used the random transmission model expression (Equation 20) to compute weighting functions for the 15μ CO_2 band for the Martian atmosphere. The weighting functions for tangent heights of 0 to 60 km, at 10 km intervals in tangent height, are plotted in Figure 2. In these computations it has been assumed that the Martian scale height is 10 km, the surface pressure is 5 mb, the surface density is $1.2 \times 10^{-5} \text{ g cm}^{-3}$, the temperature of the Martian atmosphere is 200° and the band constants are those given by Rodgers and Walshaw (1966). It is obvious from Figure 2 that for tangent heights greater than 20 km most of the energy emanates from a rather narrow vertical thickness of atmosphere, of order of 5 km. Thus, observations of 15μ band

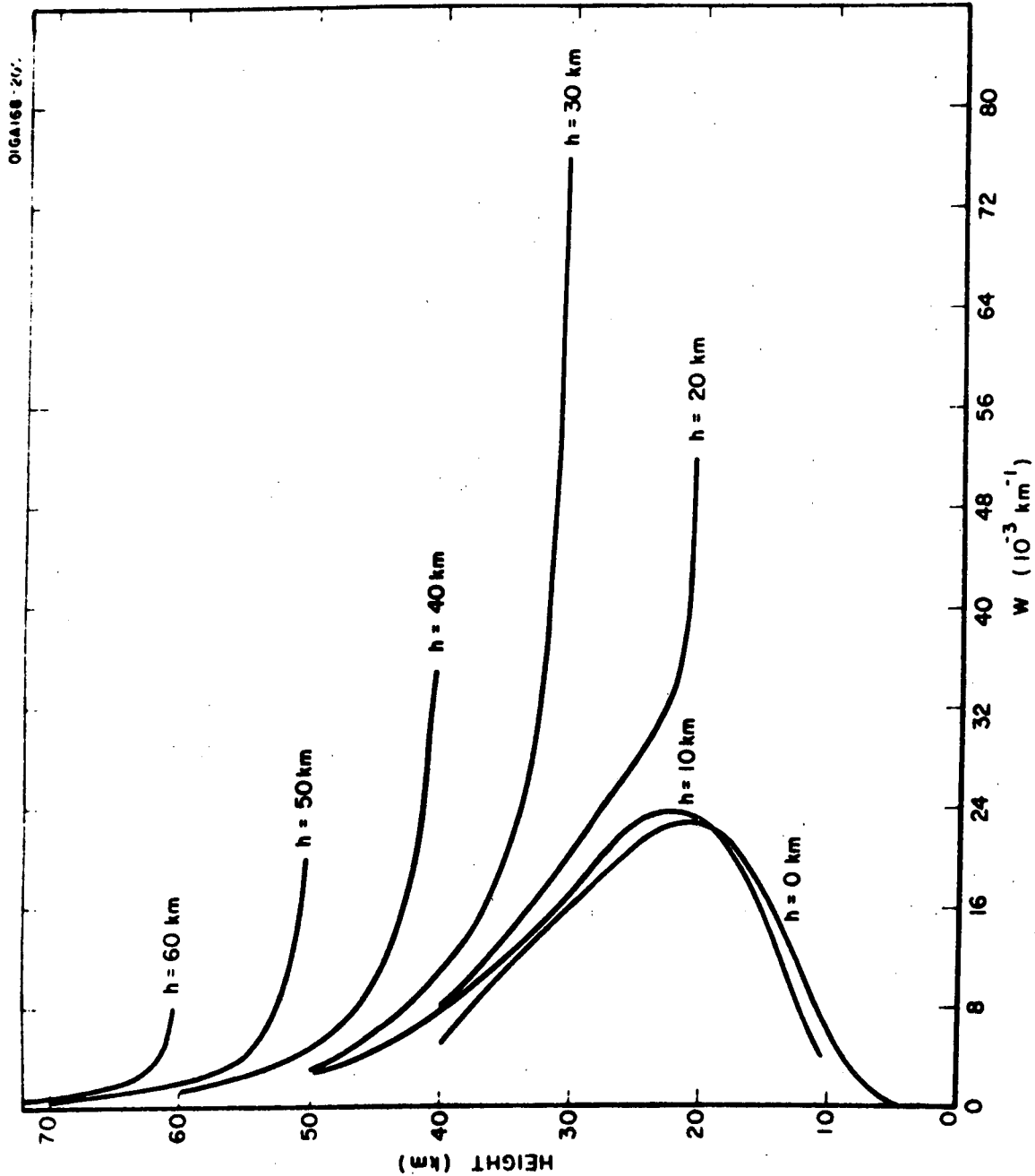


Figure 2. Mars horizon radiance weighting functions for the 15μm CO₂ band for different tangent heights, *h*.

radiance at 5 km or greater tangent height intervals are almost independent of each other and could be used to infer, quite directly, mean temperatures with 5 km vertical resolution. A rather simple technique, "instant inversion," is developed below.

From Equation (1) or (5) it can be seen that the intensity of radiation received by the radiometer can be written as

$$I(h) = \int_{\tau(-\infty, h)}^1 B \, d\tau \quad (38)$$

where $\tau(-\infty, h)$ represents the transmittance of the entire atmospheric path tangent to the Martian atmosphere at height $z = h$. The weighting functions for tangent heights greater than 20 km are such that most of the energy emanates from a rather narrow vertical interval immediately above the tangent height. Thus, the temperatures above this narrow vertical interval do not contribute significantly to the observed emission. It may, therefore, be assumed that B in the integral of Equation (38) may be approximated by $\bar{B}(h)$, which represents the integrated value of the Planck function for the average temperature of the layer immediately above the tangent height. Thus,

$$I(h) = \bar{B}(h)[1 - \tau(-\infty, h)] \quad (39)$$

The term $[1 - \tau(-\infty, h)]$ may be called the emittance, $\epsilon(h)$. Thus, one can infer $\bar{B}(h)$ from

$$\bar{B}(h) = \frac{I(h)}{\epsilon(h)} \quad (40)$$

It is a simple matter to reclaim $\bar{T}(h)$ from the integrated Planck function. Hence, the vertical distribution of temperature of the Martian atmosphere can be obtained from observations of I as a function of tangent height h .

From Equation (18)

$$\tau(-\infty, h) = \exp\left(-\sqrt{2} A e^{-h/H}\right) \quad (41)$$

The emittance of the Martian atmosphere as a function of tangent height is shown in Figure 3.

For purposes of deriving and illustrating the method, we have assumed a model isothermal atmosphere to calculate the variation of emittance with tangent height. Although the emittance varies with temperature, this is a second order effect compared to the variation of the Planck function with temperature. Hence, Equation (40) can be used to infer temperatures at different levels even though $\epsilon(h)$ is computed for an isothermal atmosphere. The effect of uncertainties in the emittance profile upon inferred temperatures can easily be examined.

Preliminary analysis of experiment feasibility indicates that it is within the state of the art. The desired vertical resolution at the tangent height is about 5 km. For a Martian orbiter at an altitude of 1000 km, this vertical resolution can be achieved with 0.1 degree vertical field of view. A similar successful measurement of the Earth's horizon radiance profile in the 15μ CO_2 band (615 cm^{-1} to 715 cm^{-1}) from a suborbital rocket flight utilized a radiometer with 0.025 degree vertical field of view (McKee et al., 1967). Expected Martian radiances in the 15μ band are of the order of 1/10 of Earth radiances (assuming stratospheric temperatures of 150K on Mars and 230K on Earth). The wider field of view suggested for the Martian experiment helps to compensate for the lower signal levels. Scan times of the order of 1 second for a complete vertical scan, as in the successful Earth experiment, are within the state of the art. The effective horizontal resolution of an individual temperature inference would be of the order of 200 km.

This analysis shows that the orbiter based horizon radiance technique is potentially a powerful tool for measuring the vertical temperature structure of the Martian atmosphere above heights of about 20 km. It would thus complement an orbiter infrared spectrometer experiment at 4.3μ or at 15μ which could be used to infer temperature profiles for the lowest 20 km of the Martian atmosphere. If one wanted to observe the temperature profile of the lowest 20 km of the Martian atmosphere with the limb radiance technique, one has only to slide the spectral interval of the radiometer to a region of slightly lower CO_2 absorption. More sophisticated inversion techniques can also be used.

D. Application to the Problem of Inferring Martian Water Vapor Mixing Ratios

For a water vapor absorption band, we may write the following expression for the observed radiance, $I(h)$, at tangent height h

$$I(h) = \bar{B}(h) [1 - \tau(-\infty, h)] \quad (42)$$

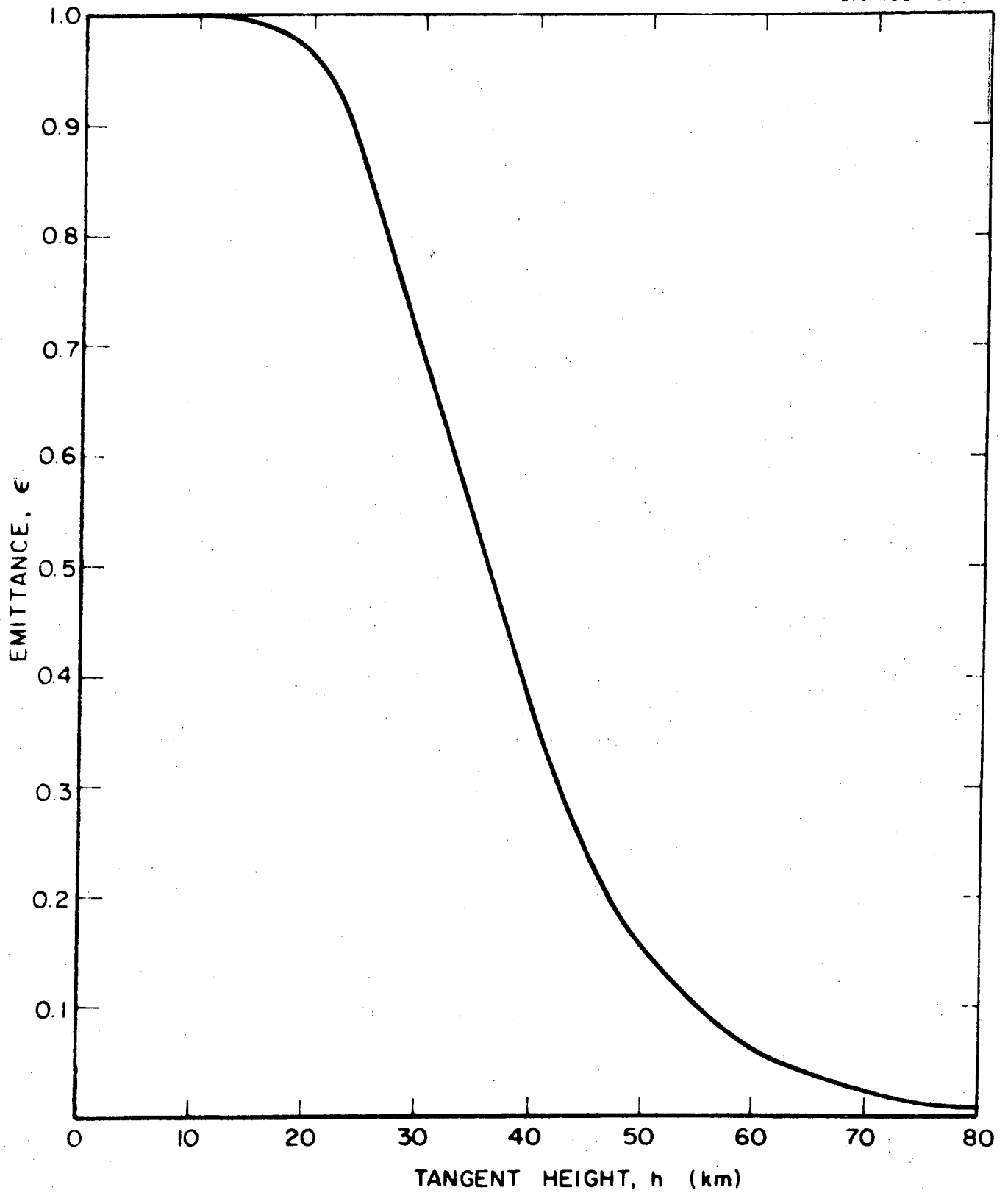


Figure 3. Emittance of the 15μ CO_2 band versus tangent height for the Martian atmosphere.

where $\bar{B}(h)$ is the integrated value of the Planck function over the water vapor spectral interval for the average temperature of the layer immediately above the tangent height, and $\tau(-\infty, h)$ represents the transmittance in the H_2O band of the entire atmospheric path tangent to the Martian atmosphere at height $z = h$. The transmittance may be written as

$$\tau(-\infty, h) = \exp\left(-\sqrt{2} A e^{-h/H}\right) \quad (43)$$

where

$$A^2 = \frac{k\pi}{\delta^2} \Phi(\theta) \alpha_s \left(\frac{p_o}{p_s}\right) \left(\frac{\theta_s}{\theta}\right)^{\frac{1}{2}} \left(\frac{\pi RH}{2}\right)^{\frac{1}{2}} \rho_o w,$$

k is the mean line intensity, δ is the mean line spacing, $\Phi(\theta)$ is a correction for the effect of temperature on the line intensities, the subscript s refers to standard temperature and pressure conditions, the subscript o to Martian surface conditions, α is the mean half-width of the absorption lines, p is pressure, θ is temperature, ρ is density, R is the radius of the planet, H is the scale height, and w is the water vapor mixing ratio. This equation is based upon the Goody random model, strong line approximation, of transmittance (see Rodgers and Walshaw, 1966, whose nomenclature and numerical values are used herein).

We have calculated the radiances, $I(h)$, for the spectral interval 160 cm^{-1} to 280 cm^{-1} in the H_2O rotational band for different water vapor mixing ratios, w . For these calculations, it is assumed that the surface pressure was 5 mb, the scale height was 10 km, and the atmospheric temperature was 200°K . The results are shown in Figure 4. The sensitivity of the radiance to the H_2O mixing ratio is clearly illustrated.

These results suggest that, if the temperature profile is known (for example, from limb radiance observations in the CO_2 band), it would be possible to obtain information on Martian water vapor from orbiter observations of the limb radiance profile in a water vapor absorption band.

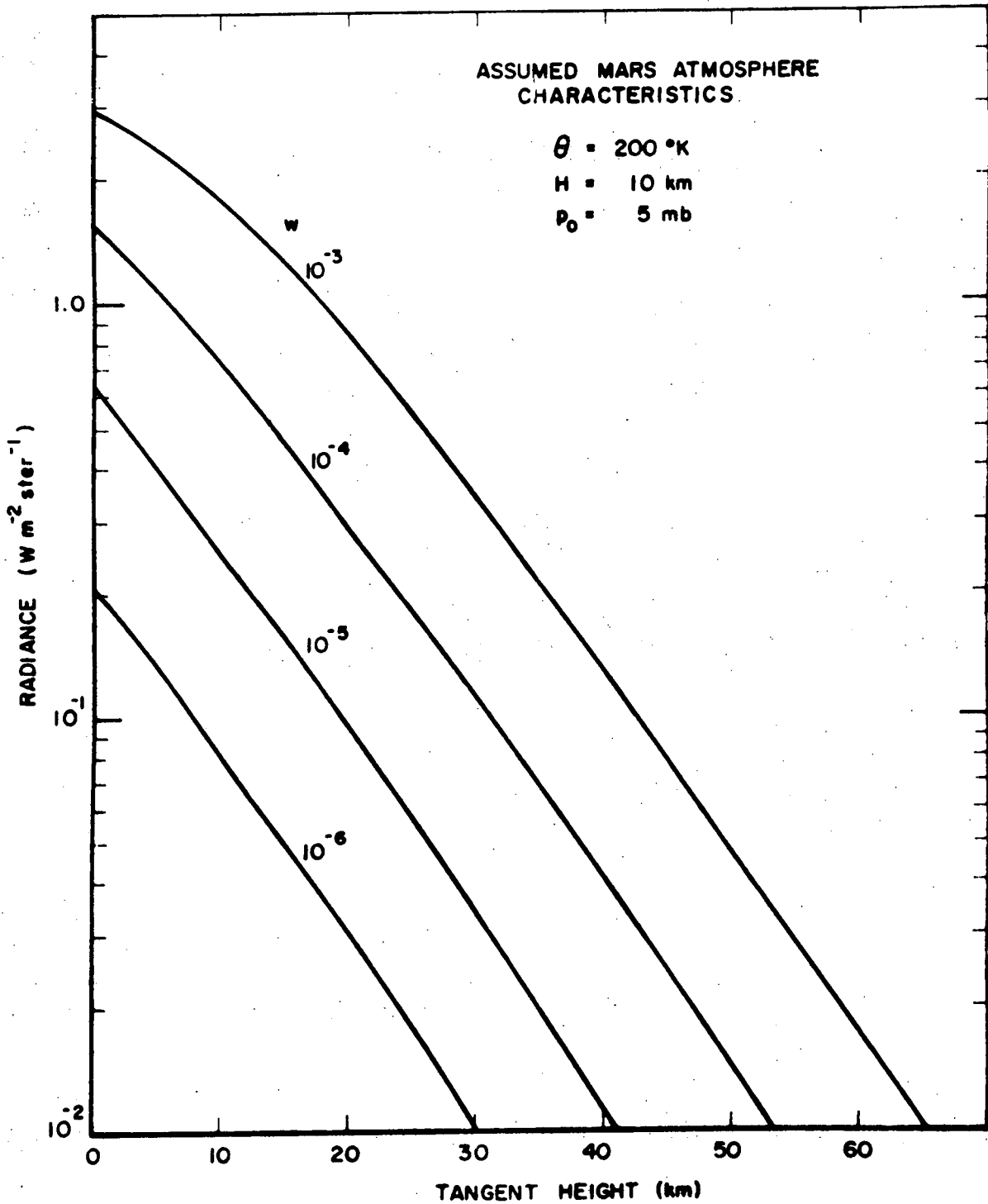


Figure 4. Calculated radiance in the 160 cm^{-1} to 280 cm^{-1} spectral region for different H_2O mixing ratios, w .

REFERENCES

- Bartko, F., and R. Hanel, Non-gray equilibrium temperature distributions above the clouds of Venus, *Ap. J.* 151, 365-378 (1968).
- Conrath, B., R. Hanel, V. Kunde, and C. Prabhakara, The infrared interferometer experiment on Nimbus 3, *J. Geophys. Res.* 75, 5831-5837 (1970).
- Hanel, R., et al., Infrared spectrometry experiment on the Mariner 9 mission: preliminary results, *Science* 175, 305-308 (1972).
- Gille, J. and F. House, On the inversion of limb radiance measurements I: Temperature and thickness, *J. Atmos. Sci.* 28, 1427-1442 (1971).
- McKee, T., R. Whitman and R. Davis, Infrared horizon profiles for summer conditions from Project Scanner, NASA Technical Note TND-5038, 31 pp. (1968).
- Rodgers, C.D. and C. O. Walshaw, 1966, The computation of infrared cooling rates in planetary atmospheres. *Quart. J. Roy. Met. Soc.* 92, 67-92 (1966).